Micropillar compression on self-irradiated and Helium implanted tungsten samples

A. Flament[1], M. Alfazzaa[2], Z. Hu[2], A. Durif[1], G. Kermouche[3], S. Kalácska[3], MF. Barthe[2]

1 IRFM, Centre CEA Cadarache, 13108 Saint-Paul-lez-Durance Cedex, France

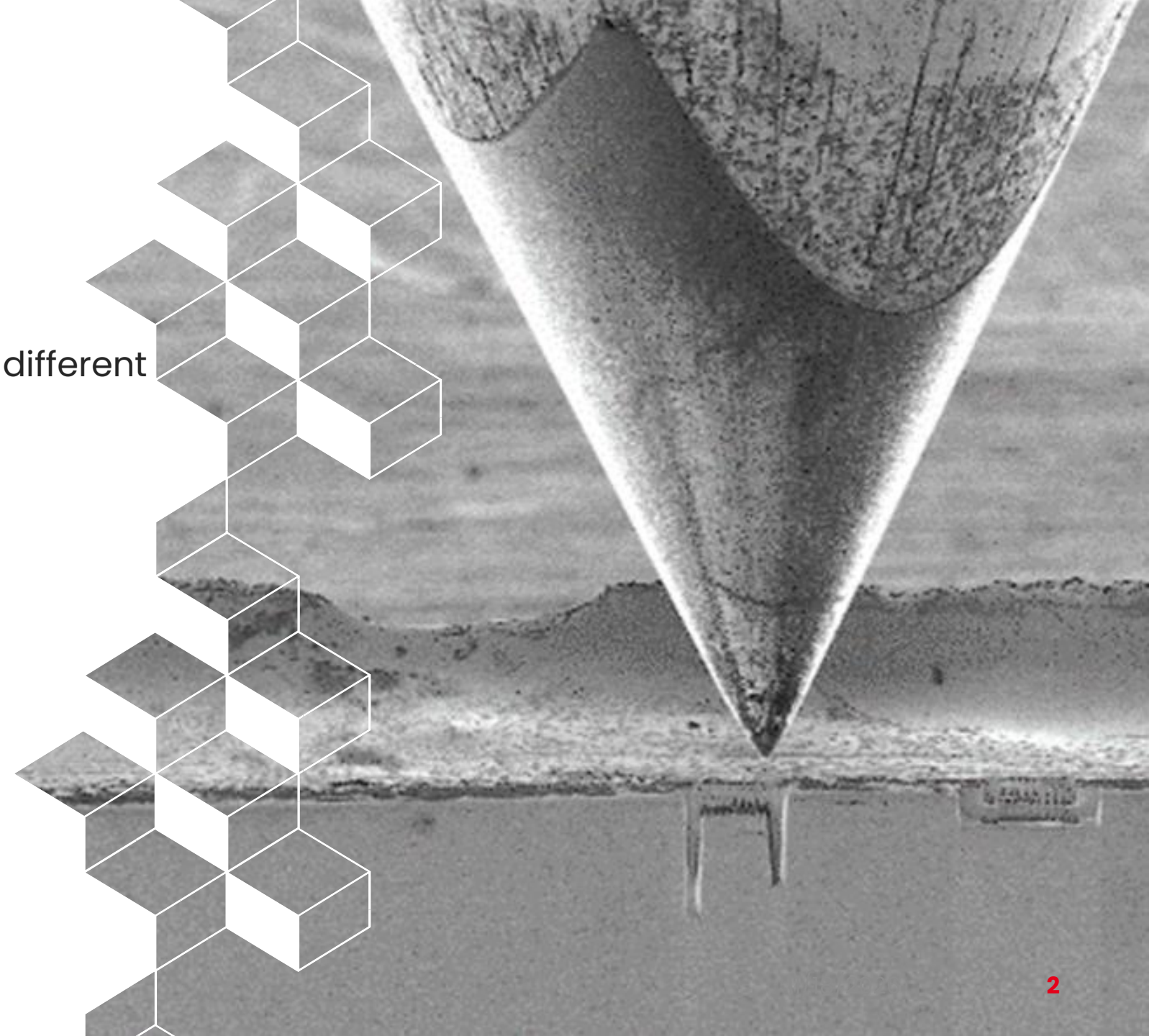
2 CEMHTI CYCLOTRON, CNRS, 3A rue de la Férollerie, 45071 Orléans Cedex 2, France

3 Ecole des Mines de Saint-Etienne, CNRS UMR 5307 LGF Centre SMS, 158 cours Fauriel, 42100 Saint-Étienne, France



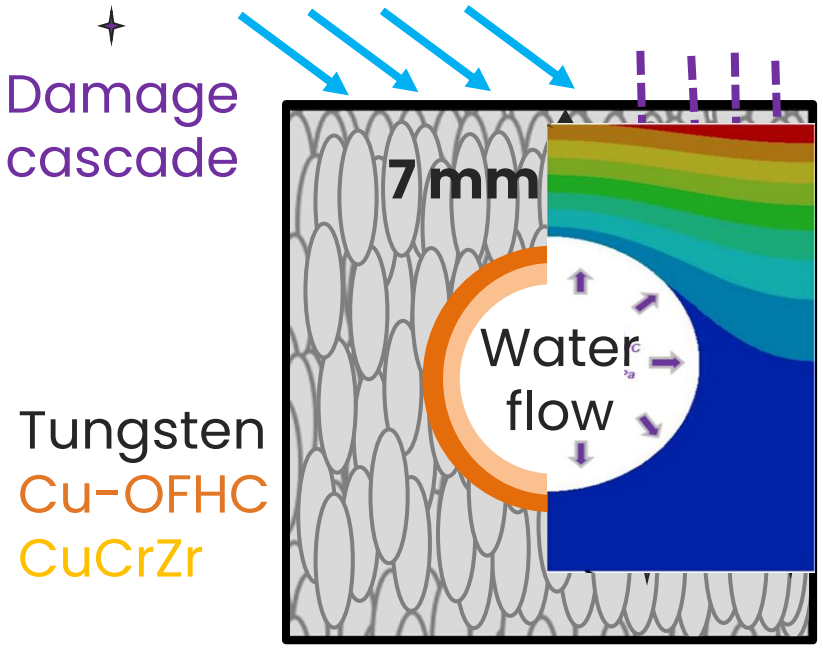
Outline

1. Context
2. Irradiation defect identification
3. Different irradiation defects induce different mechanical responses
4. Conclusion & Prospects

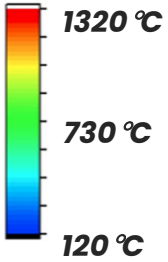


1. Context

Tokamak environment



Simplified ITER-like environment impact on Plasma Facing Components



-Plasma Wall Interaction → He, D, T,H retention

- Embrittlement [Schroeder & Ullmaier, JNM, 1991]
- Swelling [Hofmann, PIUTAM, 2016]

→ Here : Focus on Helium

-Neutron volumetric damage

- Embrittlement [Steichen, JNM, 1976][Riesch, NME, 2022]
- Hardening [Terentiev, IJRMHM, 2021]
- Reduced thermal conductivity [Cui, JNM, 2018]

-High Heat flux (Steady State : 10 MW/m²) [Chai, Vacuum, 2025]

→ Thermal gradient

Complex environment = complex lifetime estimation

PFC lifetime is related to tungsten microstructure

Plastic deformation accumulation → impact on PFC lifetime
[Durif, JNM, 2022]

At rest

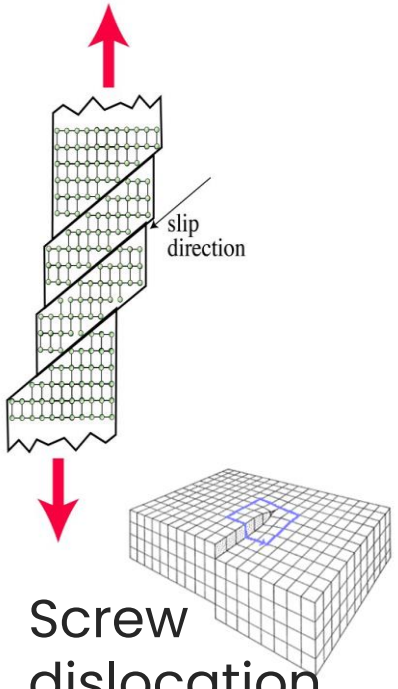


Plasma (heating)



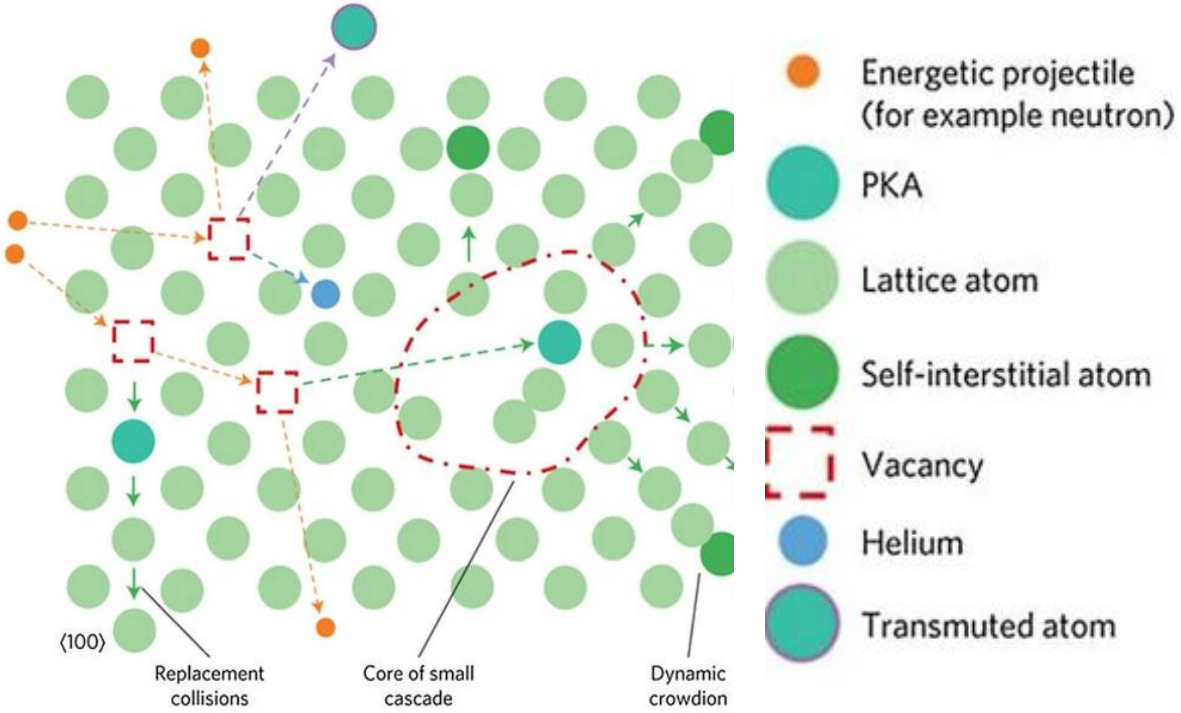
Surface compression

Plastic deformation = dislocation glide on slip planes
[Butler, IJRMHM, 2018]

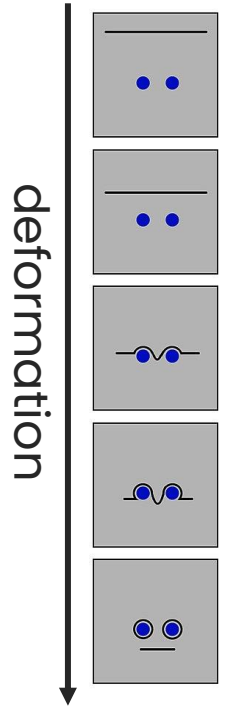


Screw dislocation

Microstructural defects created in tungsten
[Das, SN Appl. Sci. , 2019]



...can interact with dislocations



Neutron damage + Ion retention = Change in microstructure = Change in deformation behaviour = Impact on lifetime

Fuel future macroscale codes

→ For future PFC design lifetime prediction : heat loads [Durif & al., 2022] + neutron + PWI

Understand He & neutron fundamental impact on tungsten deformation

Mimic He & neutron loads with Ion Beam Irradiation…

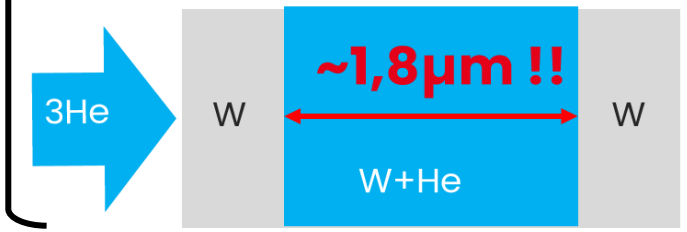
…firstly at Room Temperature

… firstly on controlled microstructure (Single Crystal, 99.999% pure)

SRIM calculations to find implantation conditions to obtain a large, ~constant damaged / implanted layer



20 MeV
~5x10^{-5} dpa/s
➔ 0.1 dpa
➔ 5x10^{13} W.cm^{-2}



0.5-1.5MeV
➔ 0.2-0.7 dpa
➔ 2x10^{16} He.cm^{-2}

Need micro scale characterization

JANNuS – Epimethée Accelerator, Saclay, France



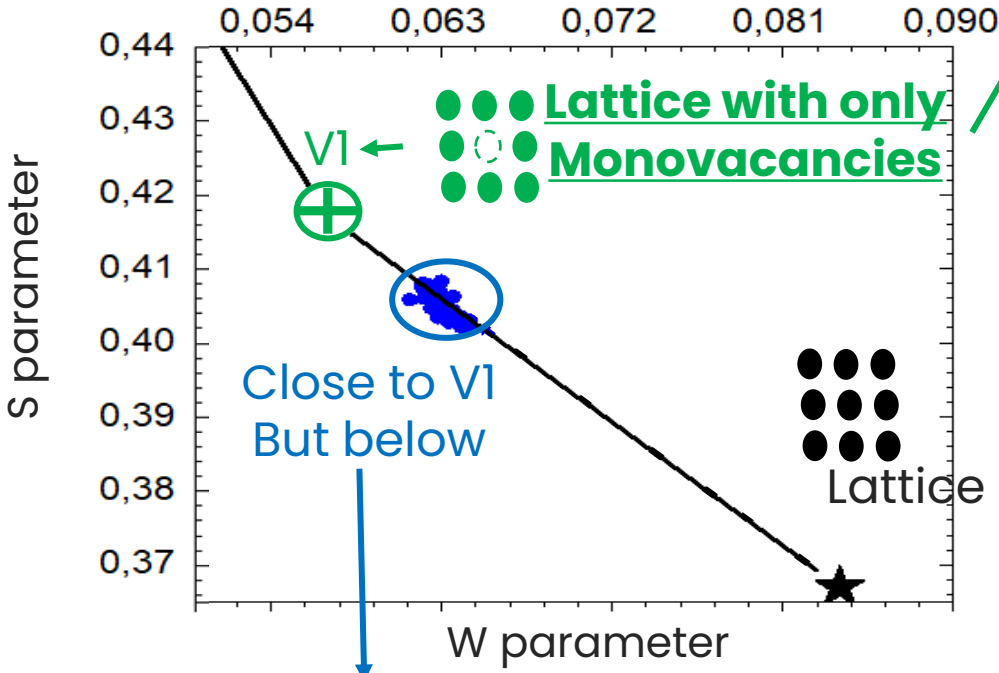
Eclair chamber – Pelletron Accelerator, CEMHTI, Orleans, France

2. Irradiation defects identification

Defect characterisation

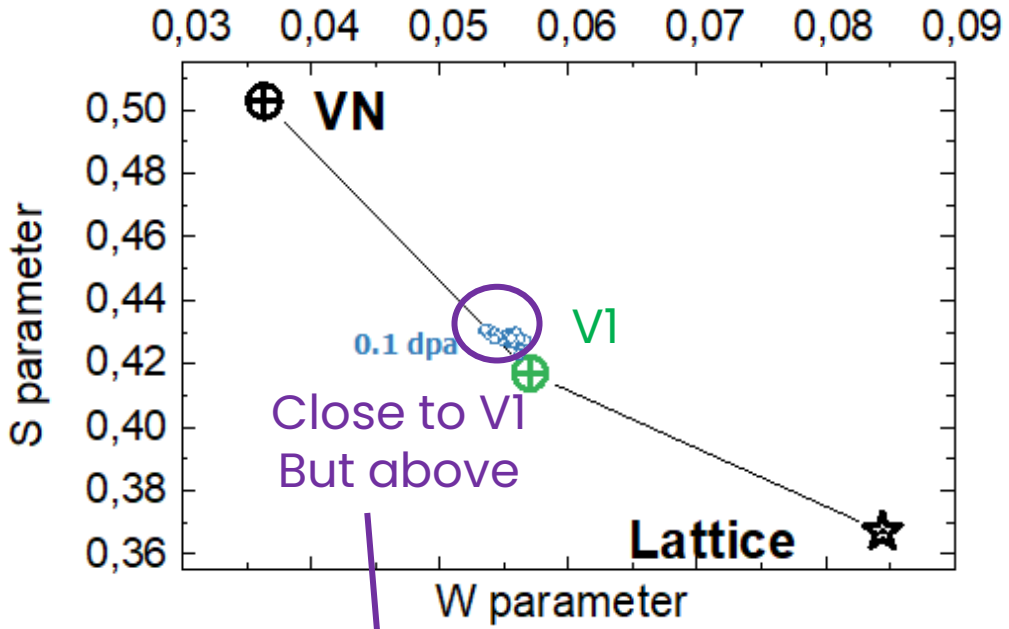
Experimental points which agree with DFT
[Hollingsworth & al., 2022]

Effect of 3He implantation



Helium implantation defects :
monovacancies
+ small He-Vacancy defects

Effect of W+ (“self”) irradiation



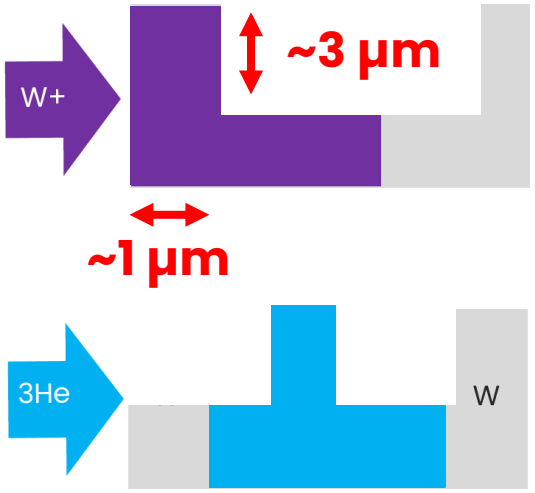
W+ irradiation defects :
monovacancies + small vacancy clusters (bi/tri-vacancies)

-Dislocation loops / Interstitial atoms ?
→ Transmission Electron Microscopy needed

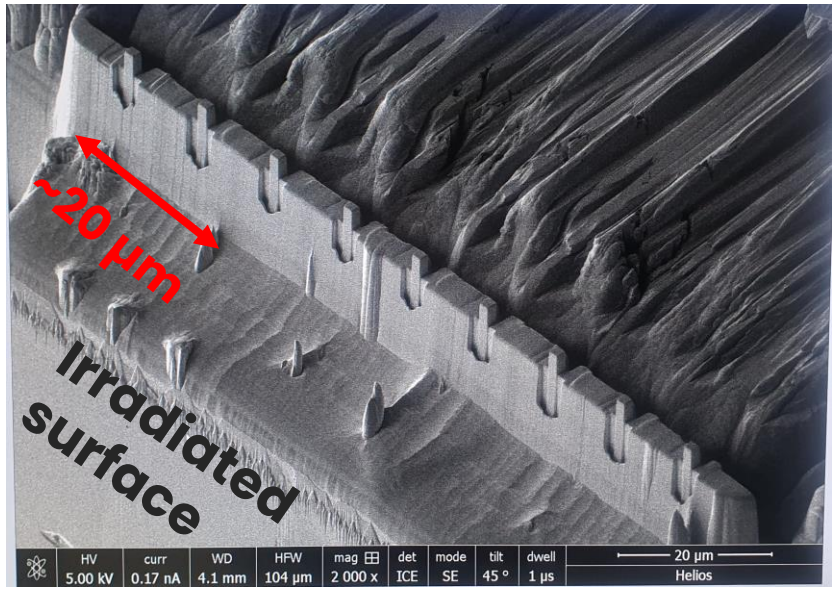
3. Different irradiation defects induce different mechanical responses

Micropillars mechanical loading

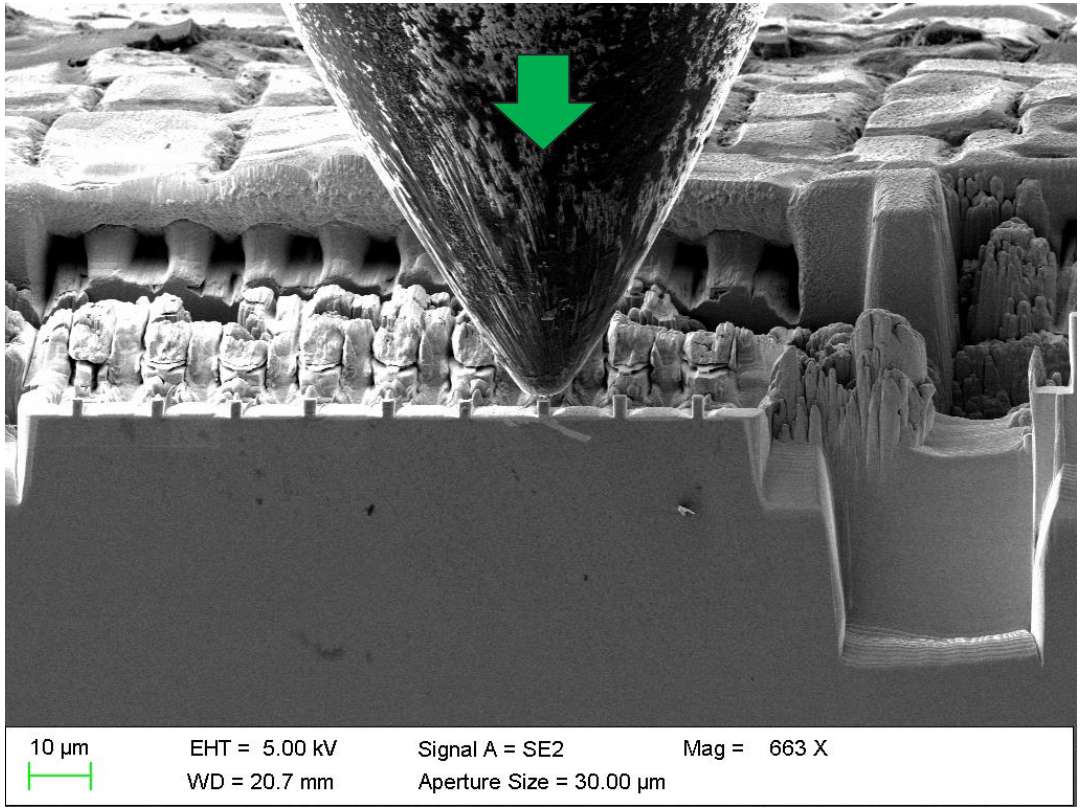
Micro-pillar created in damaged zone



Square-shaped micro-pillars prepared on tungsten sample.



Pilar compressed using a 5 µm diameter diamond flat punch



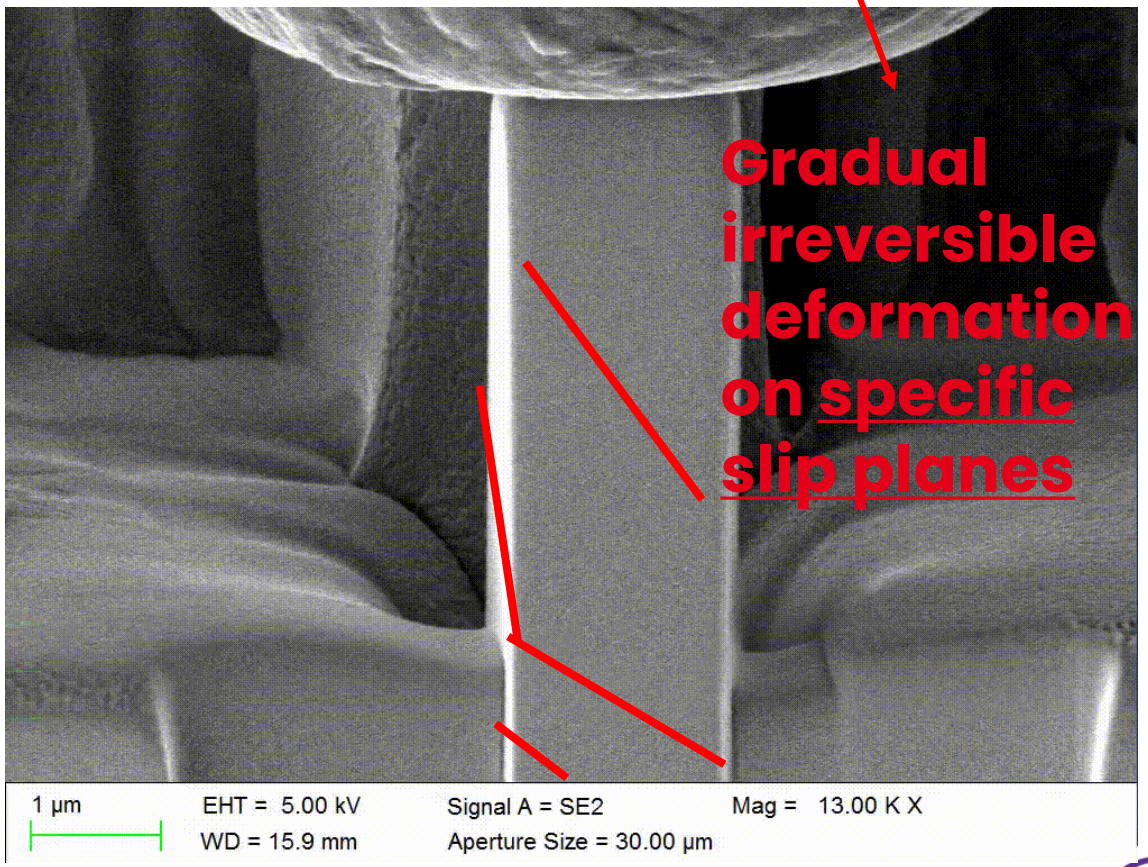
First application of micropillar compression at µm scale on He implanted / W+ irradiated monocrystaline W samples

MINES Saint-Étienne

cea

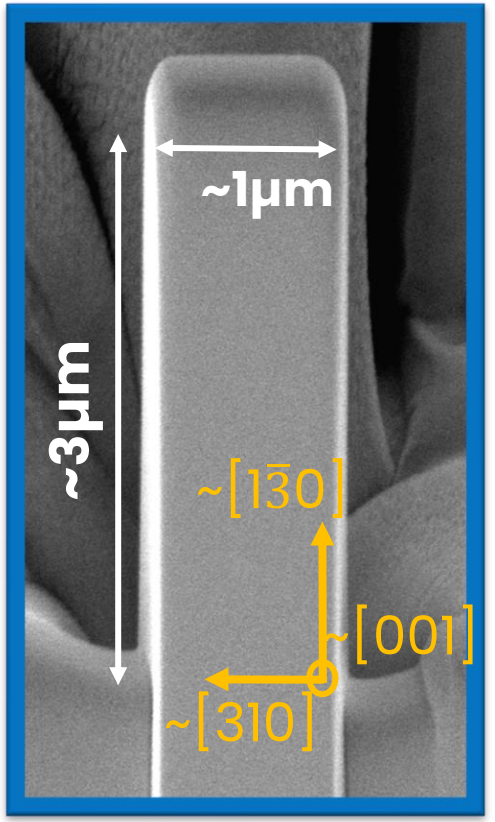
Plastic behaviour observed at micro-scale

Low strain rate ($5x10^{-3}$ s^{-1}) compression shows plastic deformation ! (not brittle)

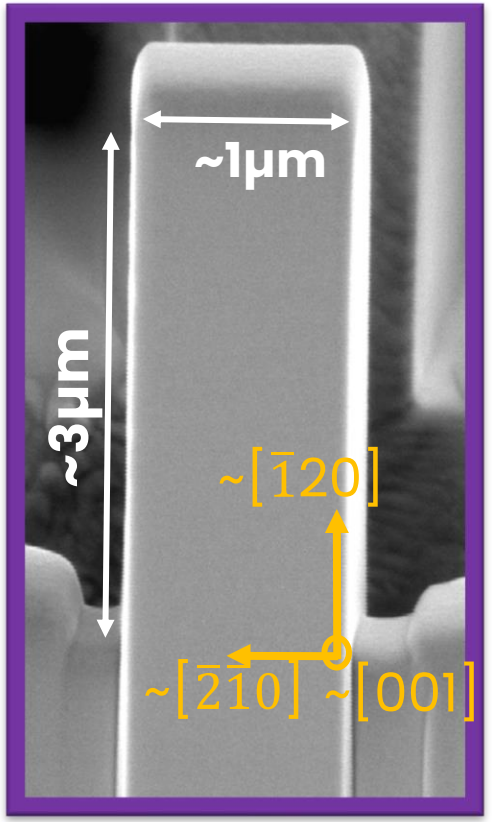


Pillar orientation determined by Electron Back-Scattering Diffraction (EBSD)

Pillars from Helium implanted sample



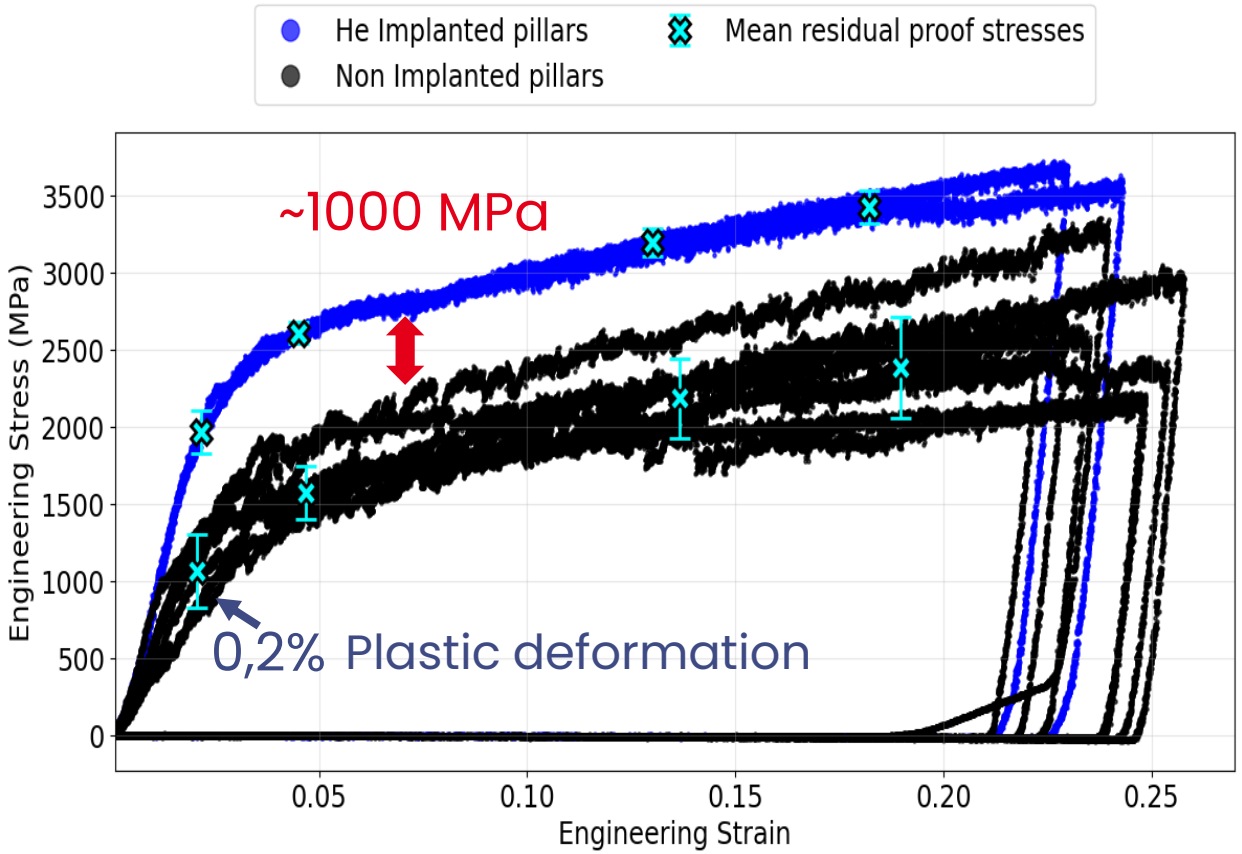
Pillars from W+ irradiated sample



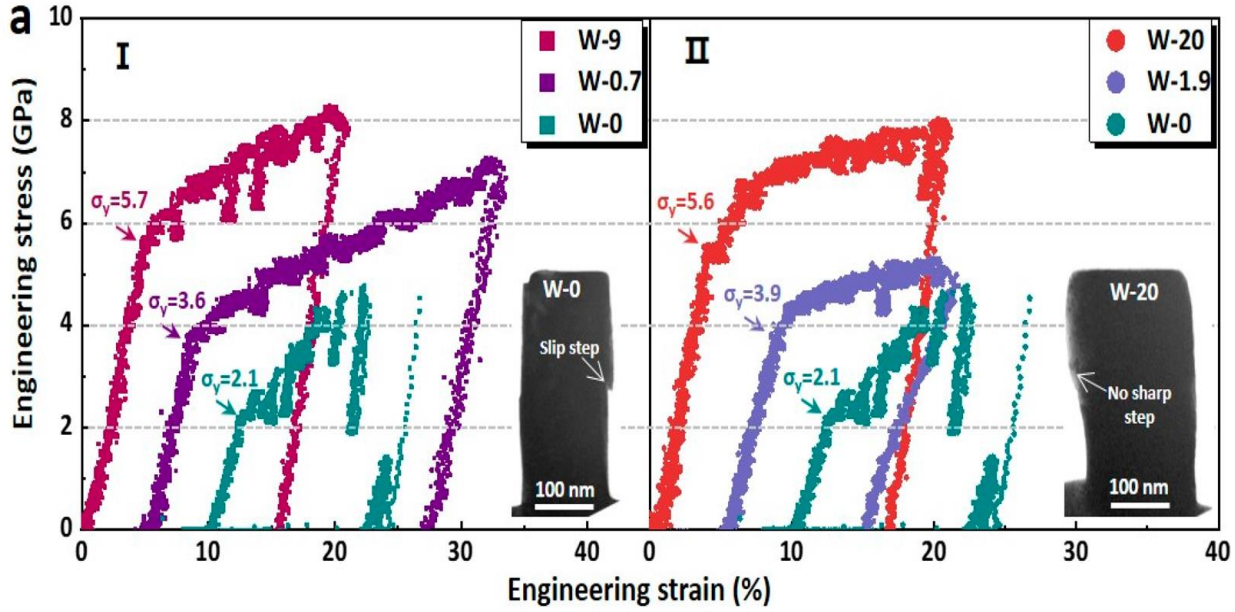
Helium induced hardening : first time at µm scale

2 pillars
8 pillars

Pillars width ~ 1µm
[He]~1.3 %at



Pillars width ~100nm
[He]~0.7-20 %at
[Zheng, Nano Letters, 2021]

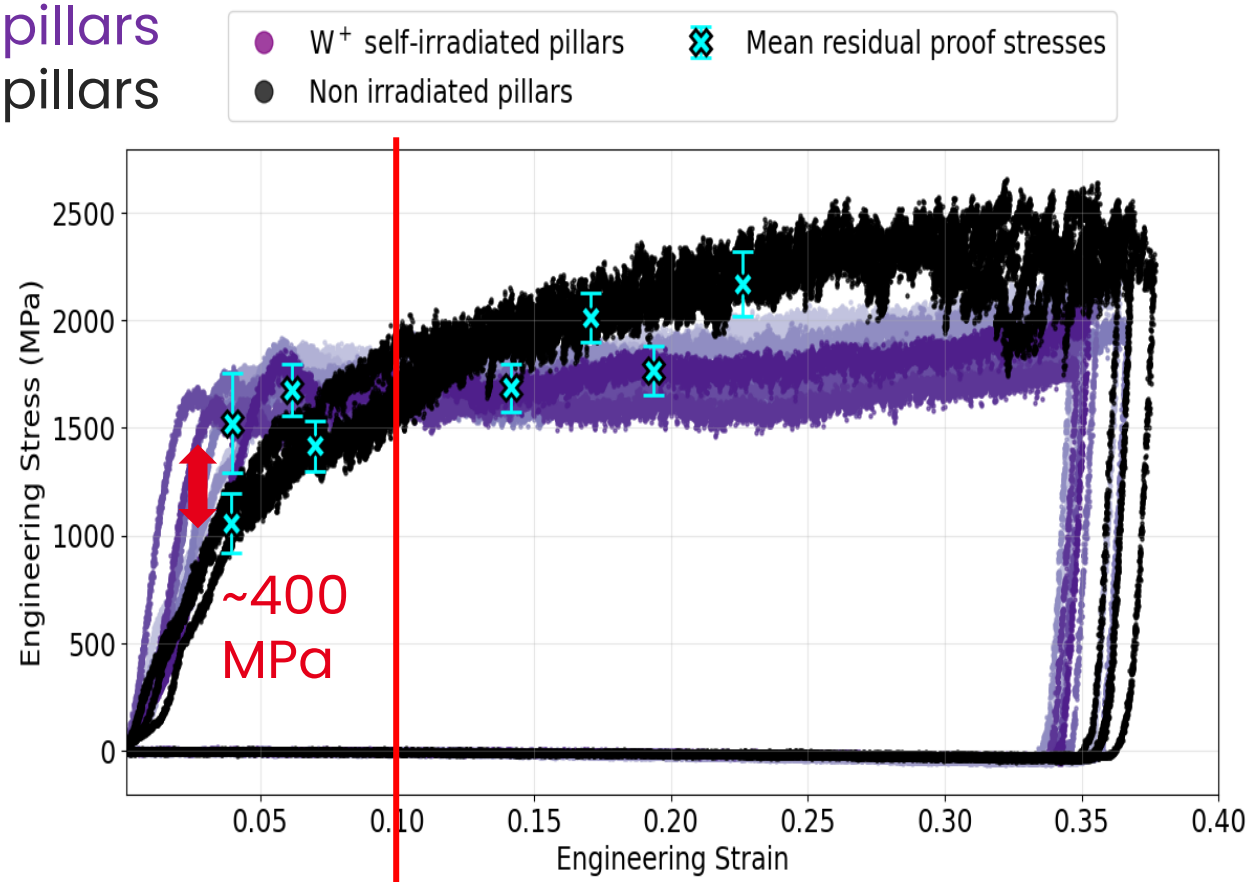


-Helium implantation induced hardening (as expected) [Zheng, Nano Letters, 2021]
-No effect on strain hardening

→ Hypothesis : He-V1(-SIA ?) defects block dislocation path but become less and less effective ? [Zheng, Nano Letters, 2021][Lin, IJP,2024][Das, JNM, 2024]

First ever self-irradiated tungsten micro-pillar compression requires more study

9 pillars
4 pillars



→ Hypothesis : Competition dislocation hardening / strain softening ? [Das, IJP, 2020]

Hardening (expected) [Hu, JNM, 2016]

-Ideal plastic behaviour = plateau
-Pristine > Irradiated (not expected → Size effect ?)

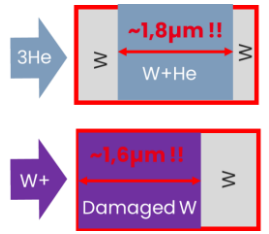
4. Conclusion & Prospects

Conclusions & Prospect

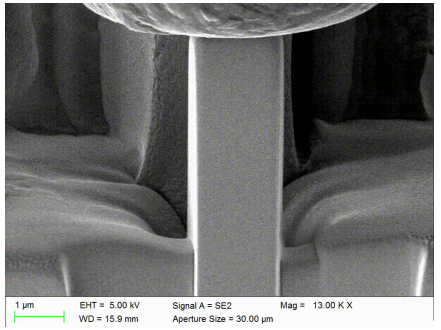
- **High availability fusion power plant need accurate lifetime prediction for Plasma Facing Component notably**

- Need to **improve our understanding regarding Tungsten damage process** (plastic behaviour) taking into account PWI & neutron induced damage

- **Ion Beam irradiation used** to mimic He & neutron induced damage in controlled conditions → **defects are induced at micron-scale**



- Different irradiation defects induce different mechanical responses :
  - Strain hardening for **Helium implanted tungsten** (0,5-1,5 MeV)
  - hardening + ideal plastic behavior for 20 MeV **W+ irradiated tungsten**



→ Need size effect study, TEM & Crystal Plasticity modeling

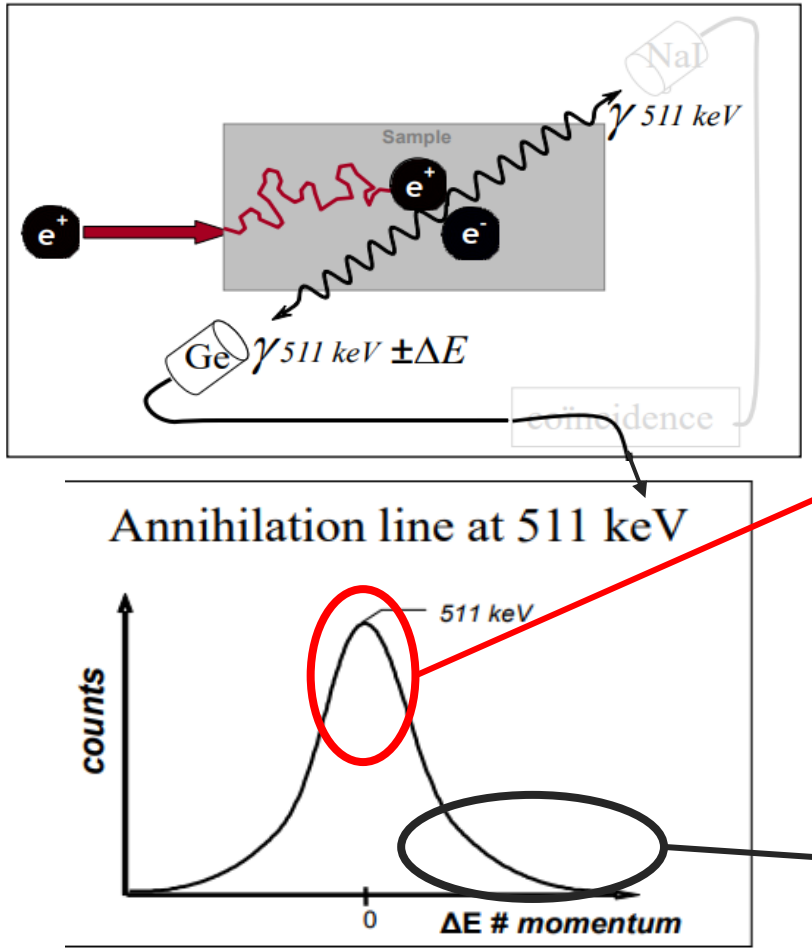
THANK YOU !



0.1. BACKUP SLIDES

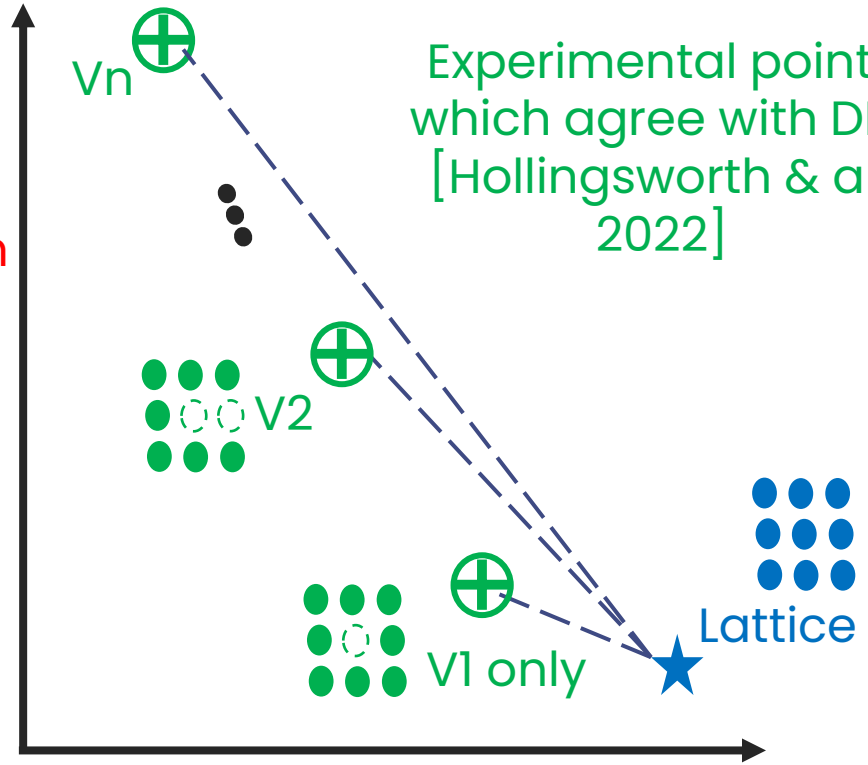
Vacancy size estimation principle

Assessment of irradiation induced vacancy size can be done



Low momentum valence e⁻

« S » Parameter = « Vacancy »



High momentum core e⁻

« W » parameter = « no vacancy »

Figure 9 : S and W parameters estimation [Barthe & al., 2016]

[10] Marie-France Barthe, Positron Annihilation Spectroscopy to Characterize Irradiation Induced Vacancy Type Defects in Materials for Nuclear Fission and Fusion, EPJ Web of Conferences 115, 03004 (2016) DOI: 10.1051/epjconf/201611503004, https://www.epj-conferences.org/articles/epjconf/pdf/2016/10/epjconf_MINOS2015_03004.pdf
[11]Hollingsworth et al JNM 558 (2022) 153373

Goal : micropillar modelling to assess irradiation defects impact on dislocation motion

From classical Finite Element Modelling…

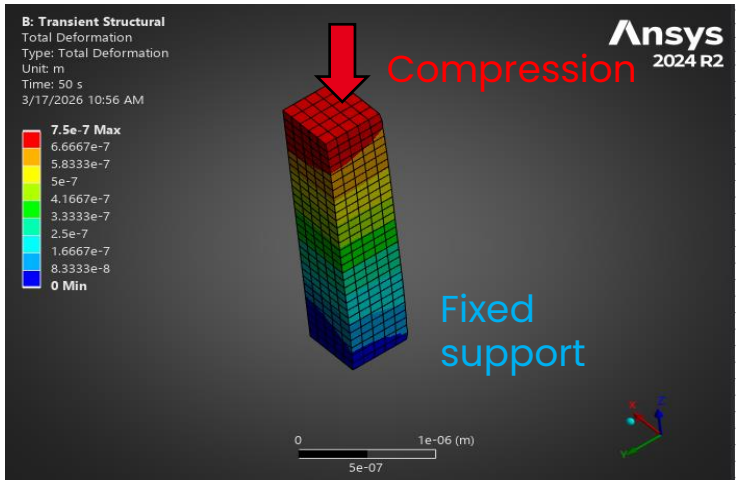


Figure 19: Ansys strain drived micro-pillar compression modelling

+

Micropillars
TEM
DB-PAS

To Crystal Plasticity Finite Element Modelling

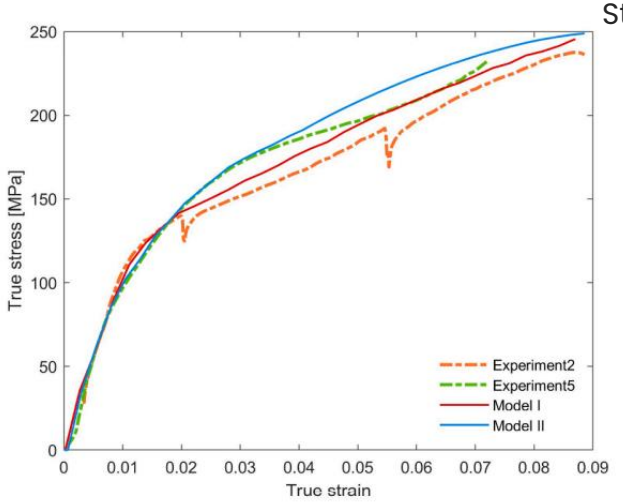


Figure 20 : Approach experimental stress-strain curves with Crystal Plasticity Finite Element Modelling [Jeong & al., 2022]

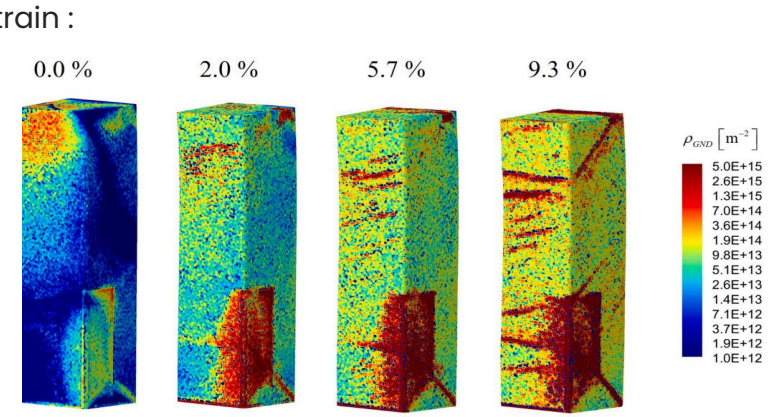
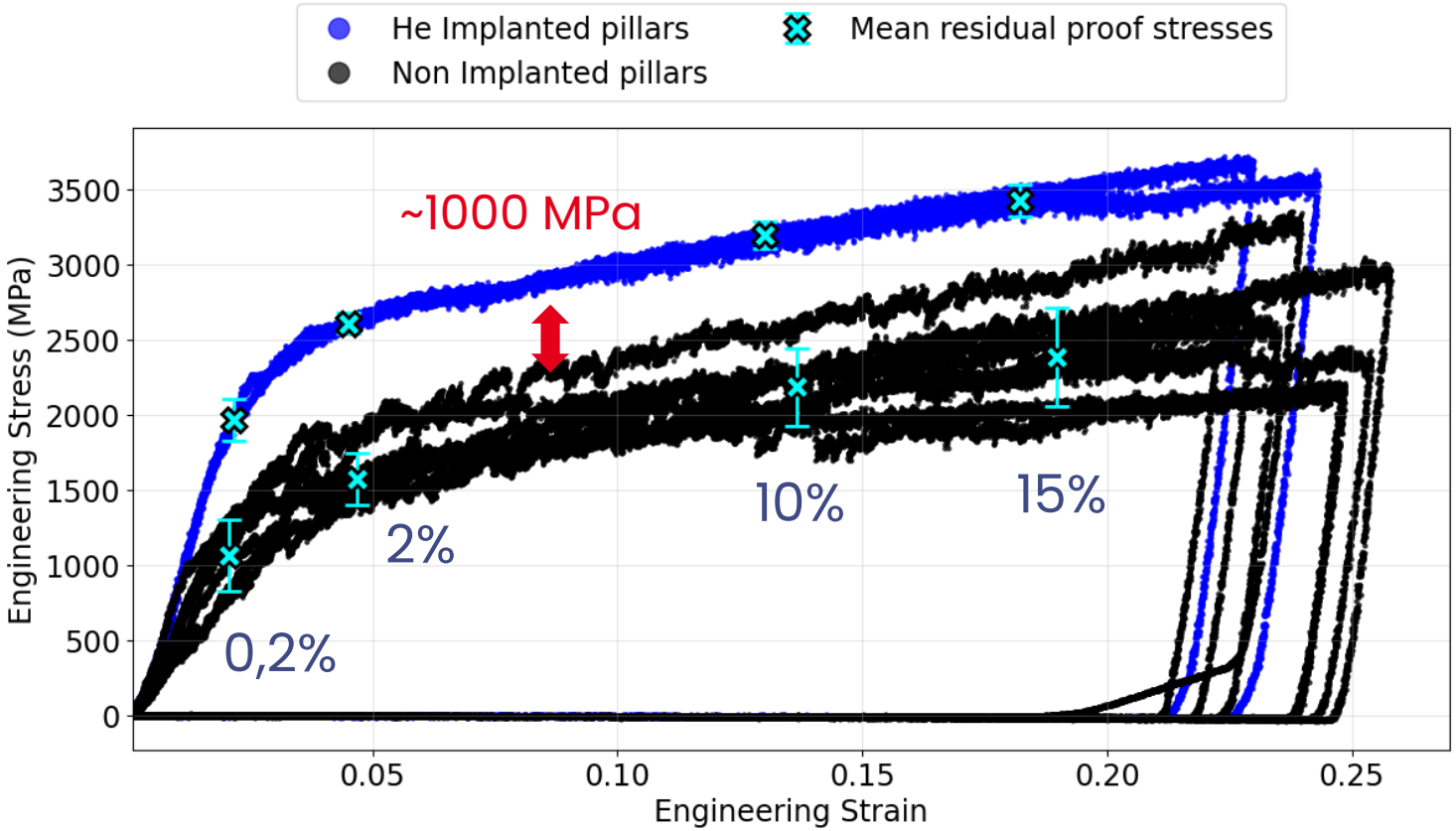


Figure 21: Example of GND dislocation assessment inside a micro-pillar during deformation using Crystal Plasticity Finite Element Modelling (CPFEM) [Jeong & al., 2022]

[13] Jeong, J. & Voyiadjis, G. Z. A physics-based crystal plsticity model for the prediction of the dislocation densities in micropillar compression. *Journal of the Mechanics and Physics of Solids* **167**, 105006 (2022).

Tungsten micropillars compression is sensitive to helium implantation…



Micropillar compression does not directly reflect macroscopical litterature values

→Tip misalignment (pillar manufacturing)

→size effect

Our work	Pristine	He implanted	Litterature
E (Gpa)	75	120	~400 (RT)
E_T (Gpa)	20	25	~0,85 (mean 500-750°C)
Rp0,2% (Gpa)	1.1	2.25	~0.54

EBSD on pillars gives more insight on pillars microstructural orientations

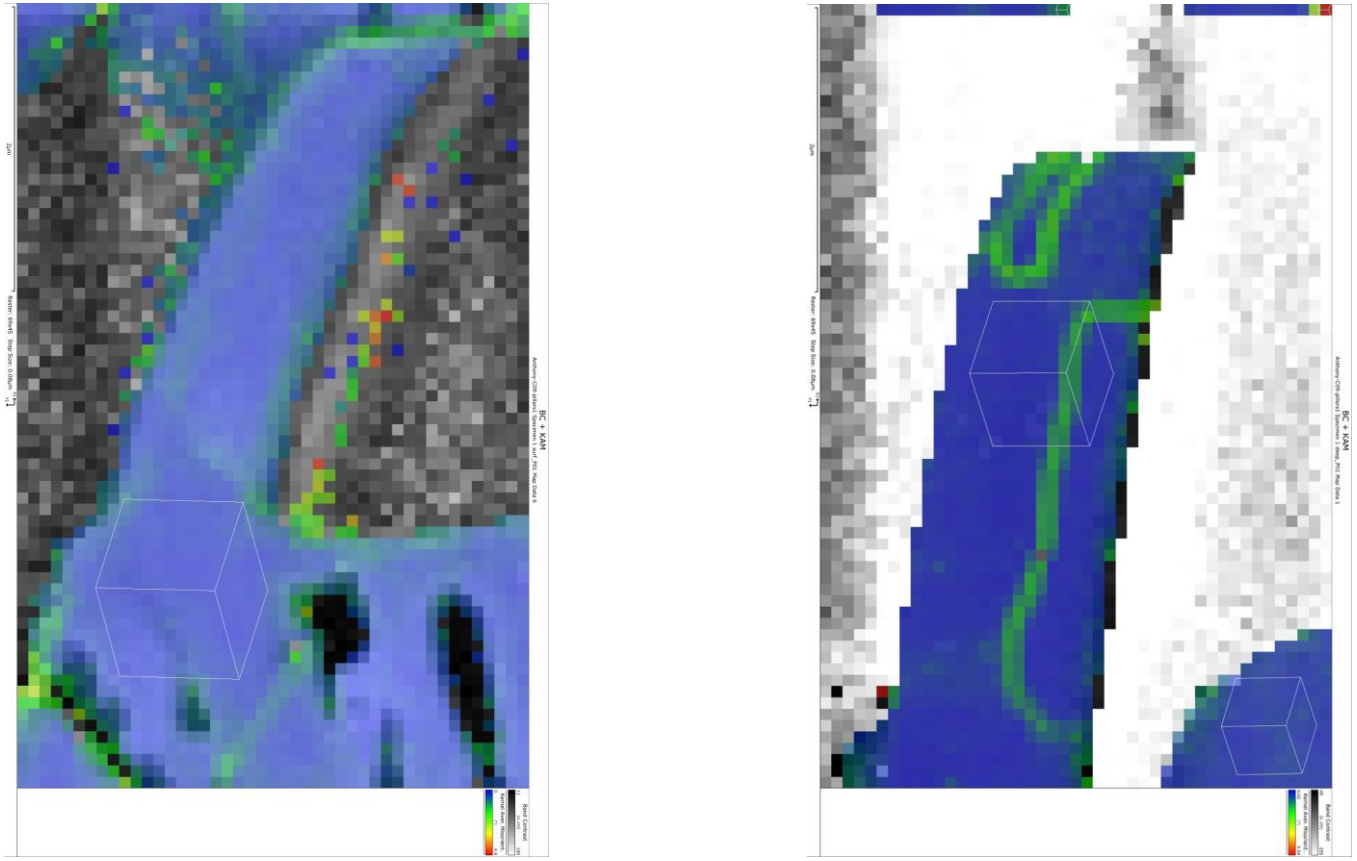


Figure 10 : Micropillars created with FIB on Polycrystal sample : ZH-W-P-GP-150-C09
Left : Irradiated pillar (surface)
Right : Non irradiated pillar (10 µm deep)

1x1x3 µm Micropillars manufactured on the side

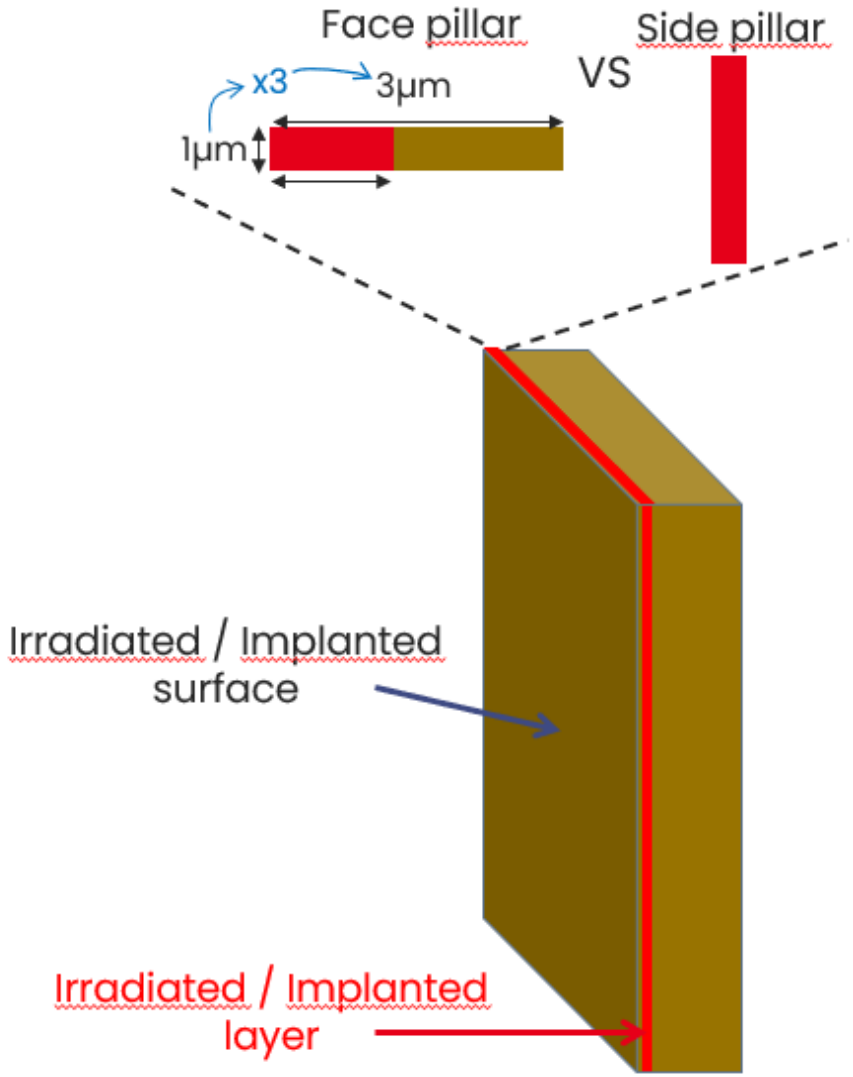


Figure 17 : Pillar orientation and location

Fission neutron damage impact on thermo-mechanical properties

Stress-strain curves modification → Yield stress modification

Fission

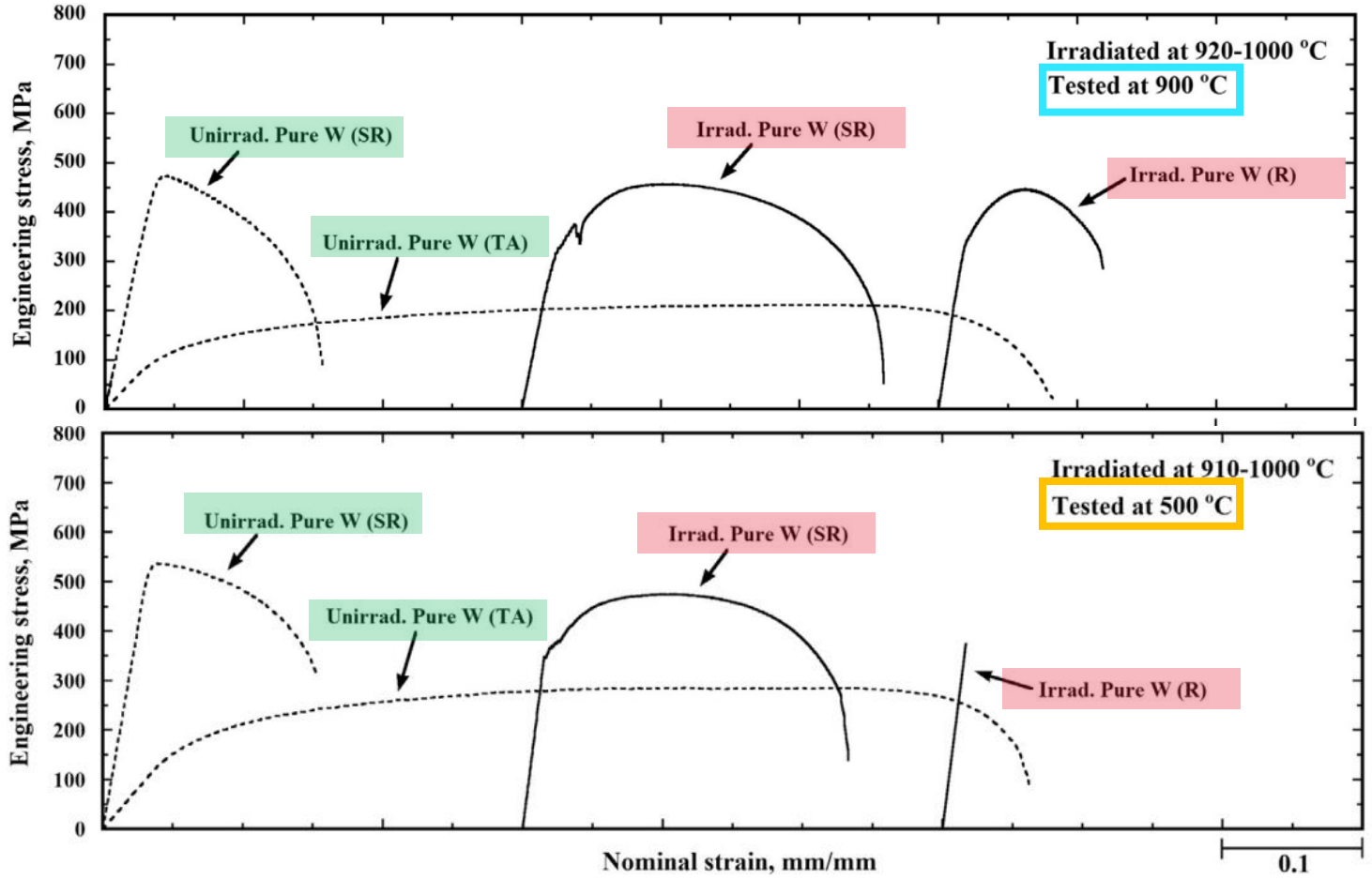
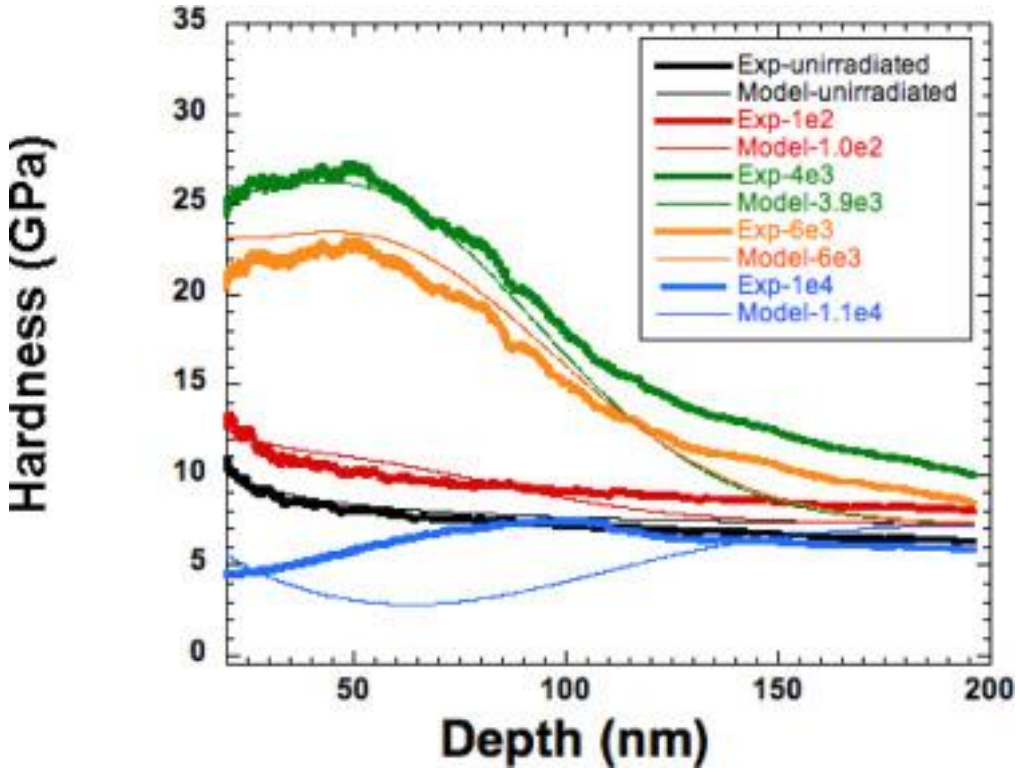


Figure 9 : Stress–strain curves of Pure W before and after irradiation at 920-1000 ℃, tested at 900 ℃ and 500 ℃ [Miyazawa, 2020]

Helium bubble impact on tungsten hardness



2 competing processes [1]

1. Hardness decrease due to the decrease in material density from bubble formation
2. Increase in hardness due to bubbles acting as pinning points that impede dislocation motion.

[1] Balooch M, Allen FI, Popovic MP, Hosemann P. Mechanical and structural transformations of tungsten implanted with helium ions. Journal of Nuclear Materials. févr 2022;559:153436.

Helium impact on stress–strain curves

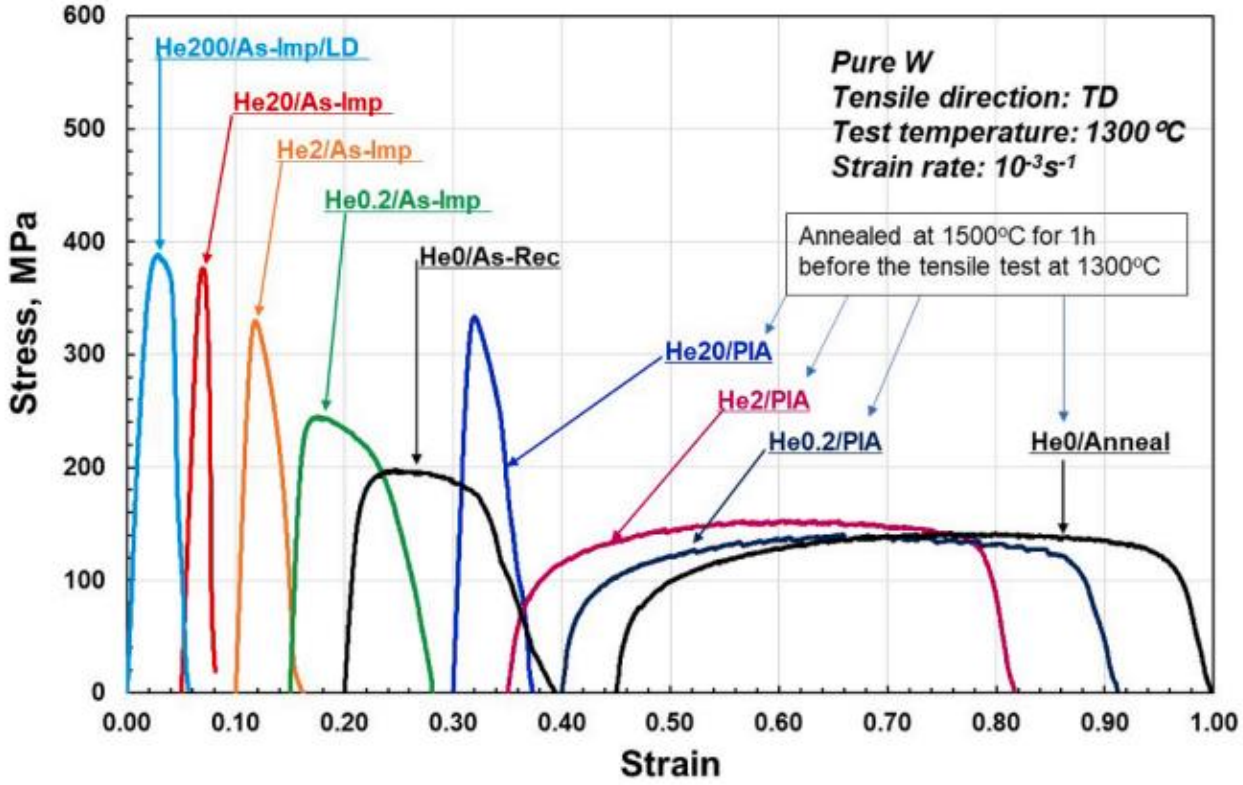


Fig. 5. Stress–strain curves of various levels of He-implanted SR-W specimens tensile tested at 1300 °C at a strain rate of 1×10^{-3} s^{-1}. The results of as-implanted or PIA at 1500 °C for 1 h specimens are shown.

[1] Hasegawa A, Sato Y, Hattori T, Kanamaru R, Du L, Miyazawa T, et al. Helium effects on tensile properties of powder metallurgical-processed tungsten for fusion reactor applications. Nuclear Materials and Energy. déc 2021;29:101076.

Representation of fusion neutron damage : comparison between fusion & fission neutron & self-irradiation

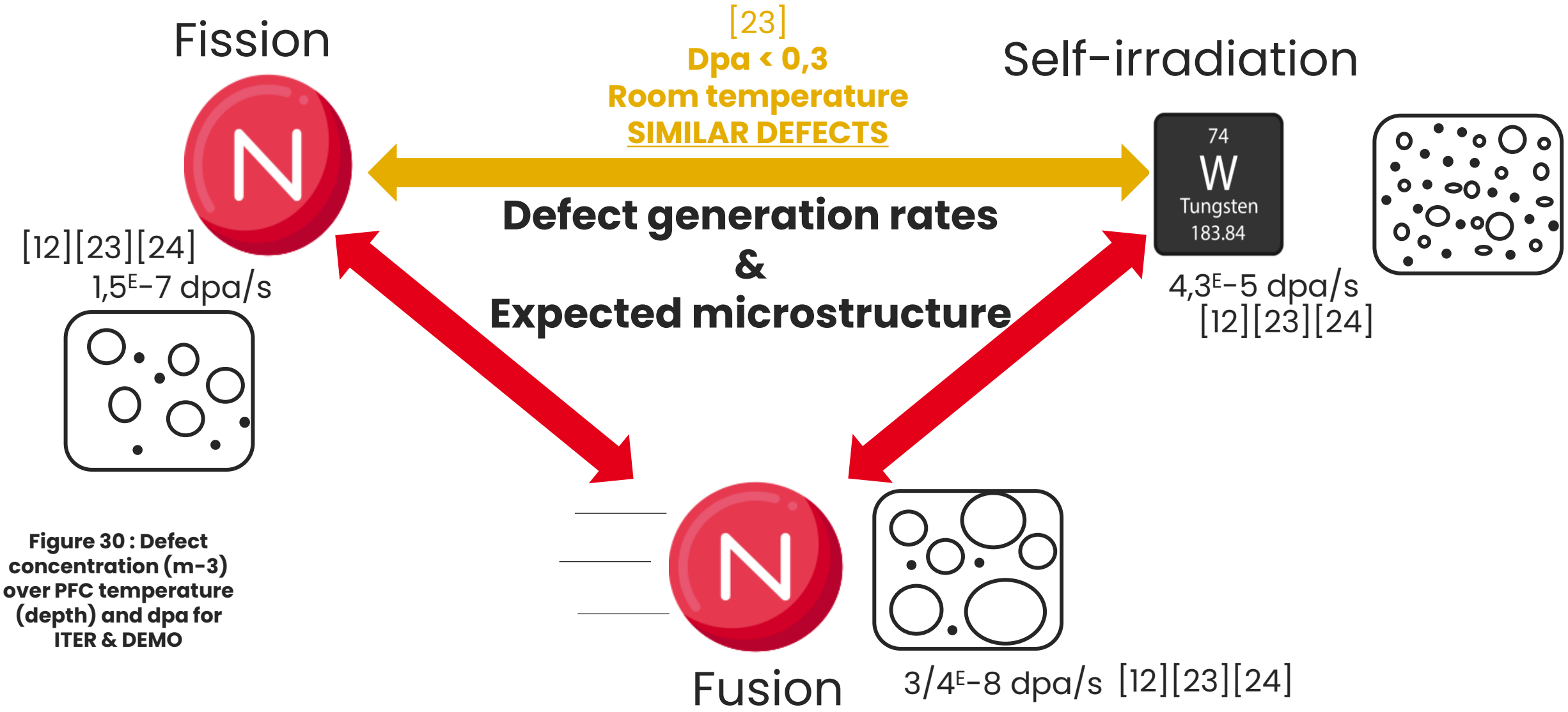


Figure 30 : Defect concentration (m-3) over PFC temperature (depth) and dpa for ITER & DEMO

[12] Mannheim A, Van Dommelen JAW, Geers MGD. Modelling recrystallization and grain growth of tungsten induced by neutron displacement defects. Mechanics of Materials. août 2018;123:43-58.
[23] Ogorodnikova, O. V.; Gann, V. Simulation of Neutron-Induced Damage in Tungsten by Irradiation with Energetic Self-Ions. Journal of Nuclear Materials 2015, 460, 60–71. https://doi.org/10.1016/j.jnucmat.2015.02.004.
[24] Hwang, T.; Fukuda, M.; Nogami, S.; Hasegawa, A.; Usami, H.; Yabuuchi, K.; Ozawa, K.; Tanigawa, H. Effect of Self-Ion Irradiation on Hardening and Microstructure of Tungsten. Nuclear Materials and Energy 2016, 9, 430–435. https://doi.org/10.1016/j.nme.2016.06.005.

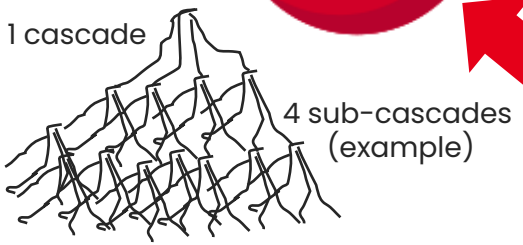
Representation of fusion neutron damage : comparison between fusion & fission neutron & self-irradiation

[23]
Dpa < 0,3
Room temperature
SIMILAR DEFECTS

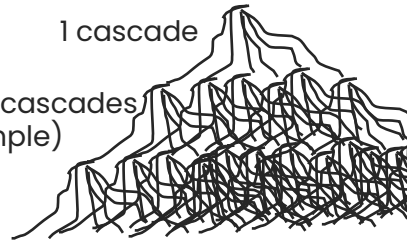
Fission

Self-irradiation

PKA
&
SUB-CASCADE
GENERATION RATES



[23]Pka < 300 keV



[23] Pka 1 MeV
+
Pka > 150 keV :
splitting

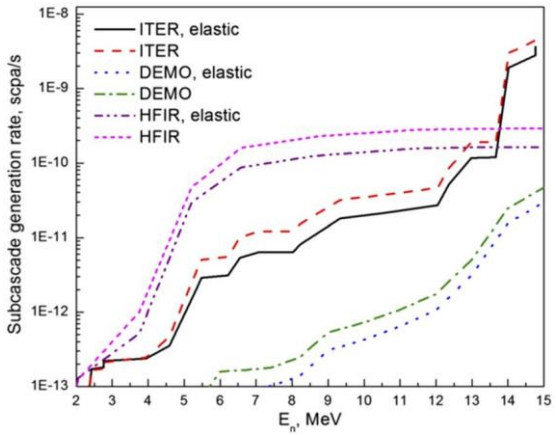
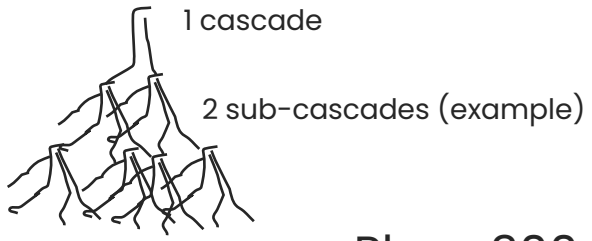


Figure 34 : Subcascade generation rate as a function of energy for fission and fusion neutrons [24]

Fusion



Pka < 300 keV [23]

[23] Ogorodnikova, O. V.; Gann, V. Simulation of Neutron-Induced Damage in Tungsten by Irradiation with Energetic Self-Ions. Journal of Nuclear Materials 2015, 460, 60–71. https://doi.org/10.1016/j.jnucmat.2015.02.004.
[24] Das S. Recent advances in characterising irradiation damage in tungsten for fusion power. SN Appl Sci. déc 2019;1(12):1614.

ITER & DEMO microstructure reproduction on test samples

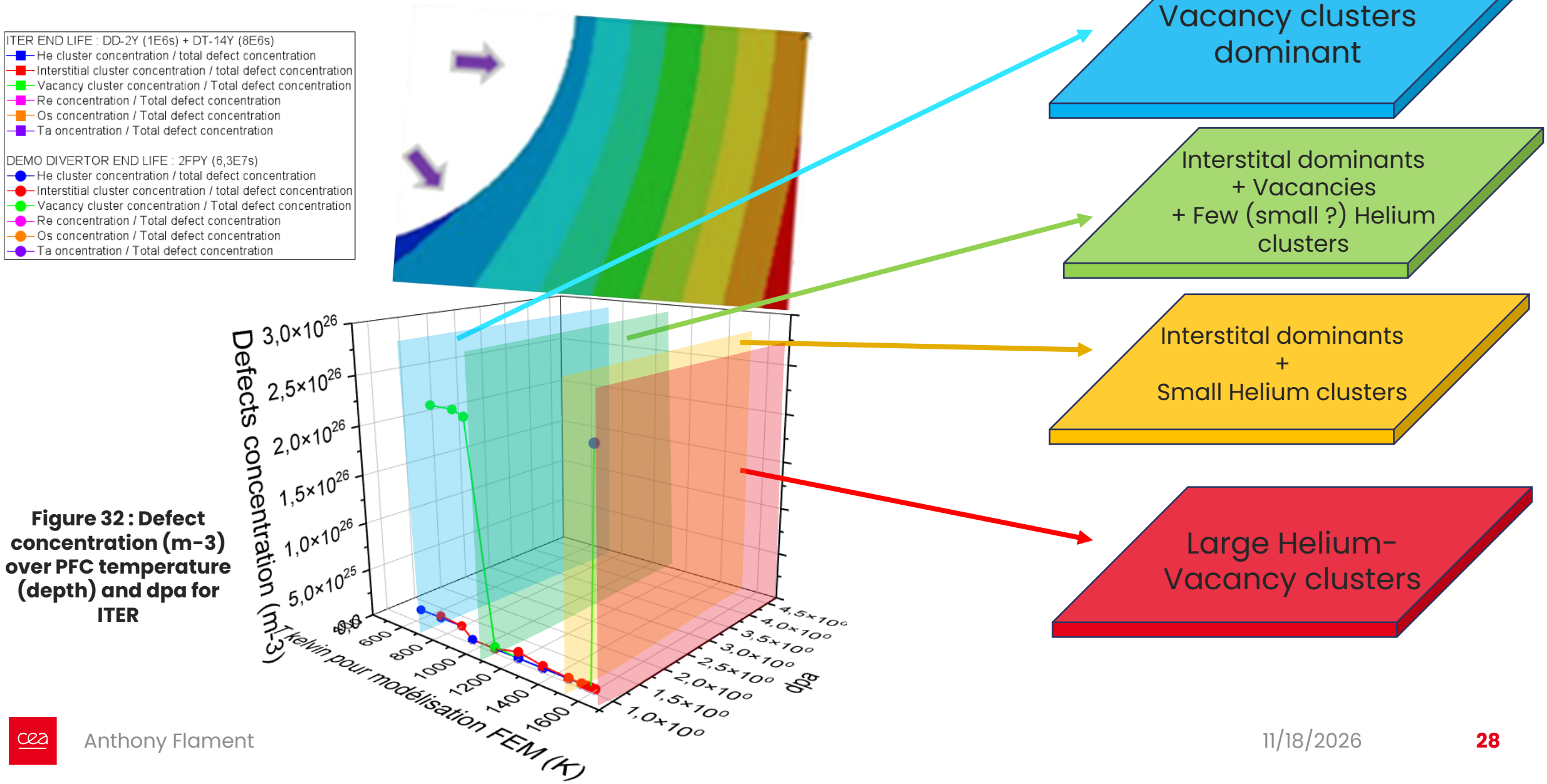


Figure 32 : Defect concentration (m-3) over PFC temperature (depth) and dpa for ITER

Nuclear Reaction Analysis (NRA) – CEMHTI (Orléans)



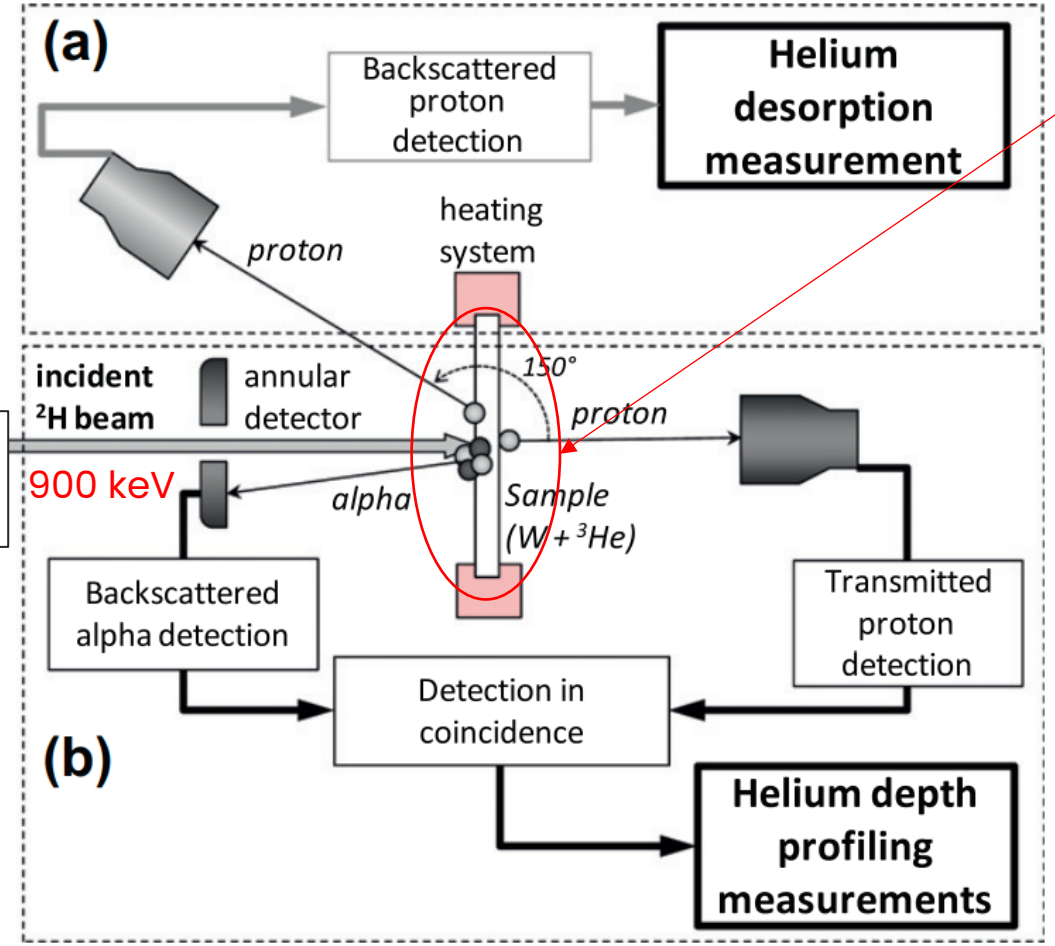


Pelletron (replaces Van de Graaff accelerator)





Principle of NRA



D + ^{3}He → α + p : Nuclear reaction

CEMHTI-Cyclotron laboratory

P.E. Lhuillier, 2013, Helium retention and early stages of helium-vacancy complexes formation in low energy helium-implanted tungsten, Journal of Nuclear Materials 433 (2013) 305–313, http://dx.doi.org/10.1016/j.jnucmat.2012.09.001

X. Templates

How to gradually approach the characterisation of ITER load conditions ?

1 **Understand PWI & neutron fundamental impact on tungsten deformation**

↓

Mimic PWI & neutron with Ion Beam Irrradiation firstly at Room Temperature on controlled microstructure

↓

Micropillar Compression

2 ? **•••**

-Higher temperature ?
-Higher fluence ?
-Higher dpa ?
-Crystal orientation dependency ?

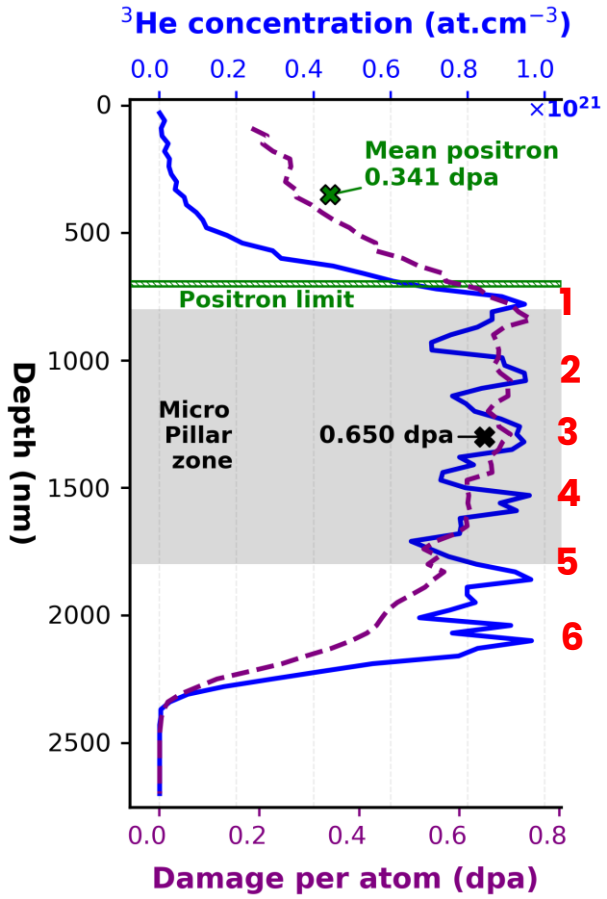
Goal

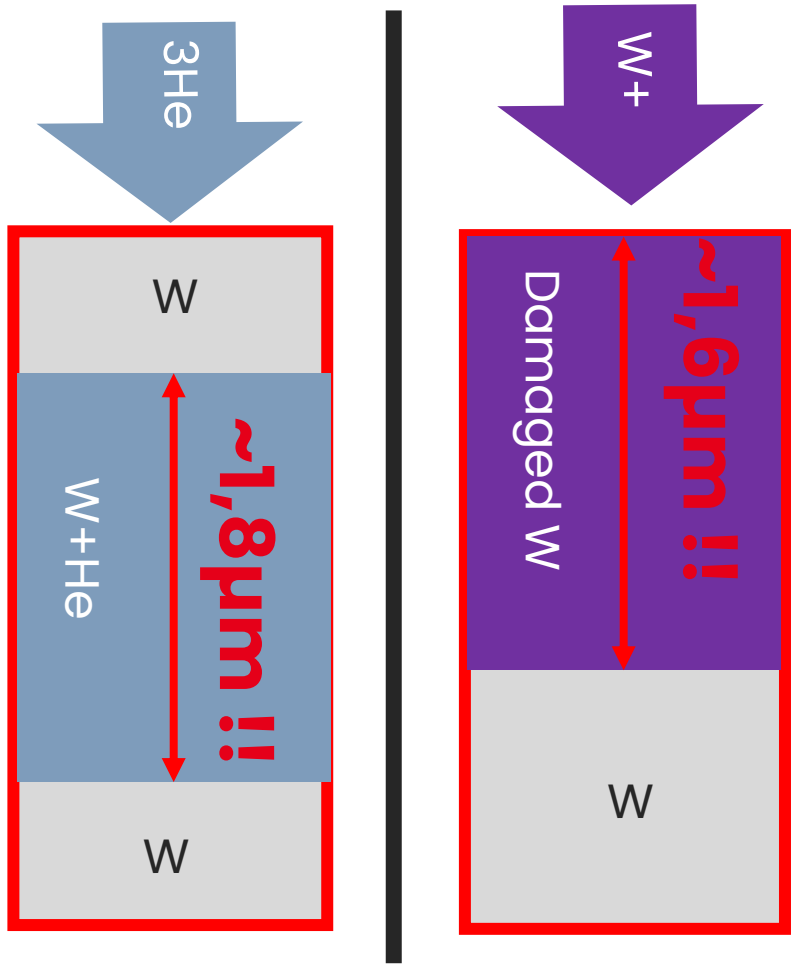
- **Macroscale plasma facing component lifetime estimation**
- **Design improvement**

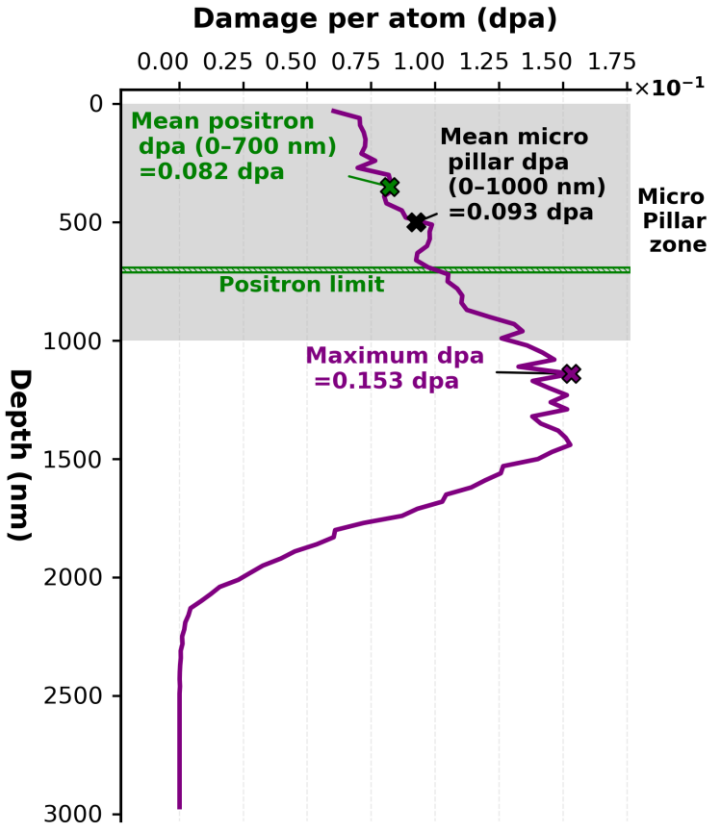
Polycristal
Impurities

~1300°C at PFC surface
-Fusion neutrons damage
-Ions (He, D, T) retention

But… ion Beam irradiation induces defects at micron scale !







micron scale

2. Mimic the effect of Helium & neutron

Light ion implantation is commonly used to mimic Plasma Wall Interaction effect in tungsten

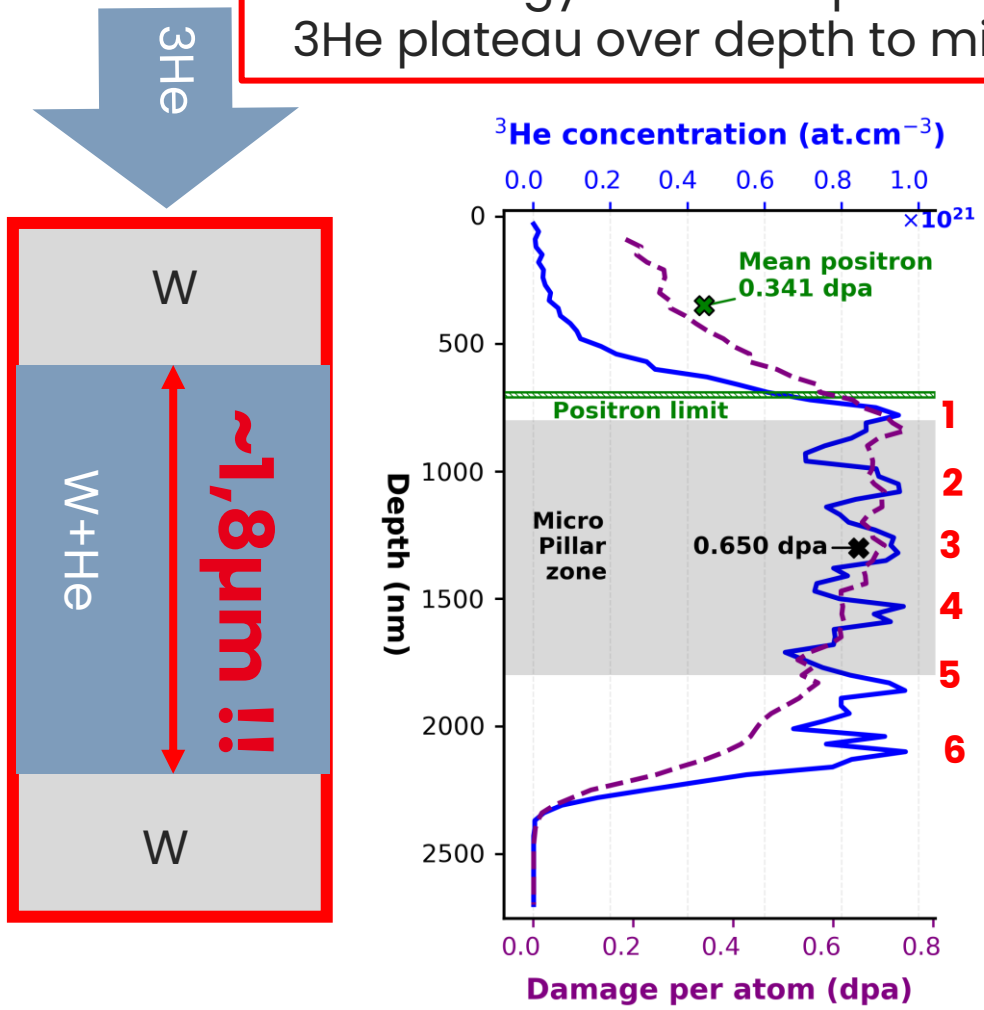
Sample 1 :
« Helium implanted sample »

7x7x0.5 mm^3
Single Crystal
99.999% pure

<u>3He implantation</u>
0.5-1.5MeV (0.2-0.7 dpa)
Room Temperature

	ITER (expected)
Temperature (°C)	1000-2000 at monoblock surface **[3]**
Damage Per Atom (dpa)	~1 at divertor end life **[10]**
Helium fluence ($at.m^{-2}$)	10^{28-30} <u>at divertor end life</u> **[11]**

Multi-energy helium implantation permits to obtain a ~1.8 µm large 3He plateau over depth to mimic helium ion retention in tungsten



Peak	Fluence ($at.cm^{-2}$)	Implantation energy (MeV)
1	$2x10^{16}$	0,5
2	$2x10^{16}$	0,7
3	$2,3x10^{16}$	0,9
4	$2,2x10^{16}$	1,1
5	$2,15x10^{16}$	1,3
6	$3x10^{16}$	1,5

Figure 7 : SRIM profile calculation to obtain a 3He plateau over sample depth

Heavy Ion Beam irradiation (W+ « self » irradiation) can be used to approach neutron effect in tungsten

Sample 2 :
« Self-irradiated sample »

Single Crystal
99.99% pure

20 MeV W+ self irradiation

- → Room Temperature
- → W+ flux : $2.5.10^{10}$ $W.cm^{-2}.s^{-1}$
- → Irradiation time : 2000s
- → Dose rate : ~5.10^{-5} dpa/s

	ITER (expected)
Temperature (°C)	1000-2000 at monoblock surface **[3]**
Damage Per Atom (dpa)	~1 at divertor end life **[10]**
Helium fluence ($at.m^{-2}$)	10^{28-30} at divertor end life **[11]**

20MeV irradiation permits to simulate neutron damage on a ~1.6 µm layer over depth

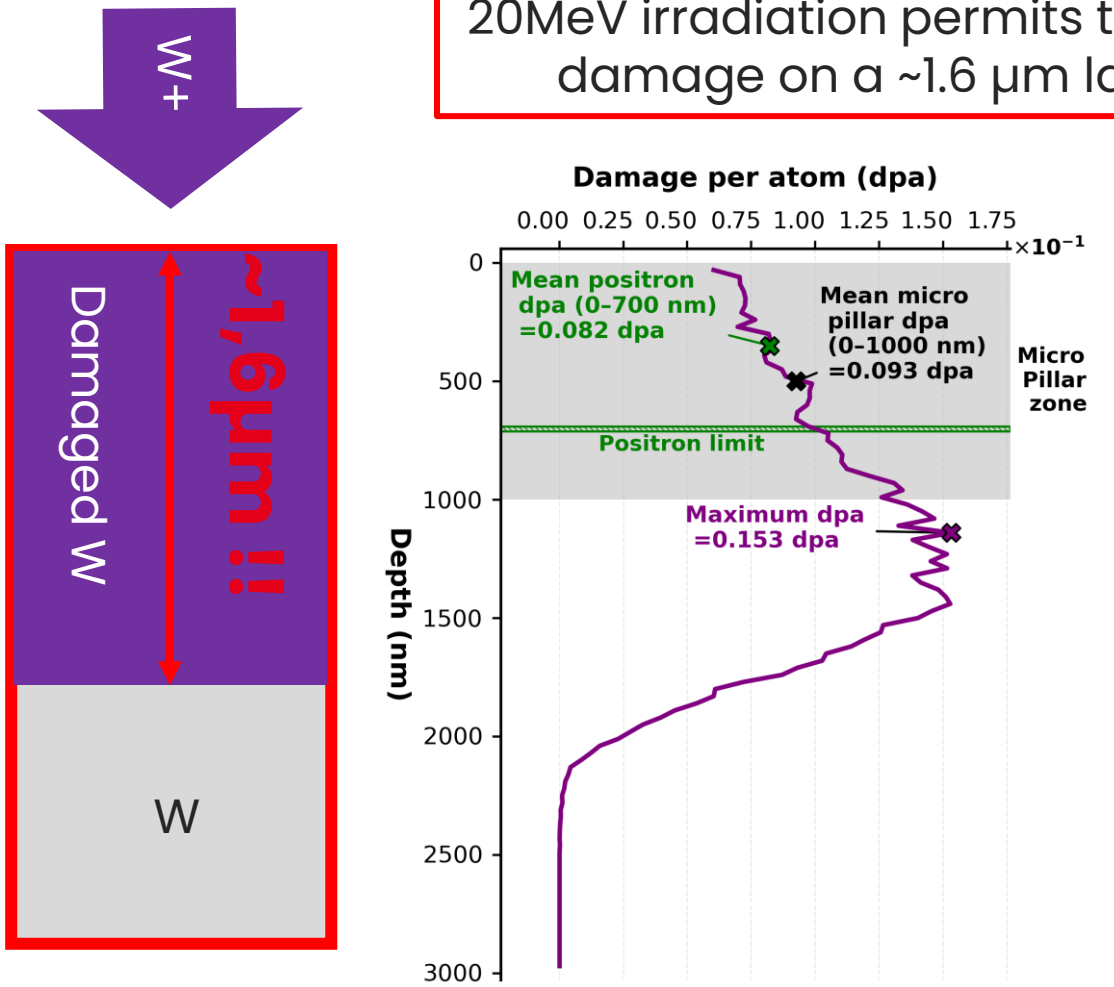


Figure 8 : SRIM profile calculation for W+ self-irradiation at 20 MeV

ITER tungsten divertor Plasma Facing Components (PFCs) design

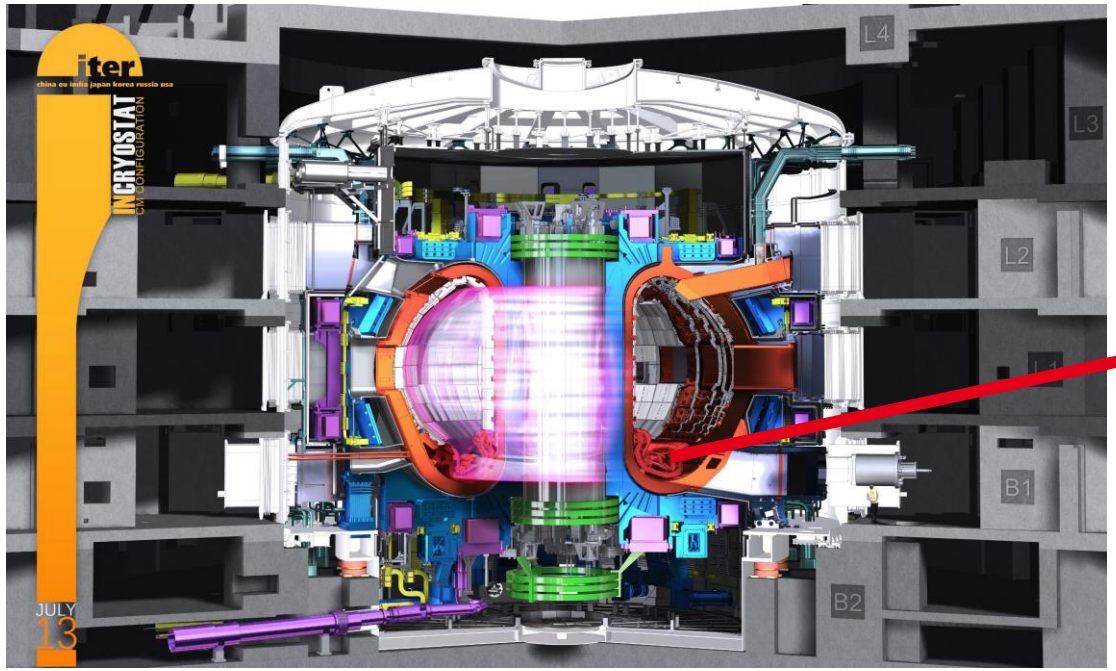


Figure 1 : ITER [1]

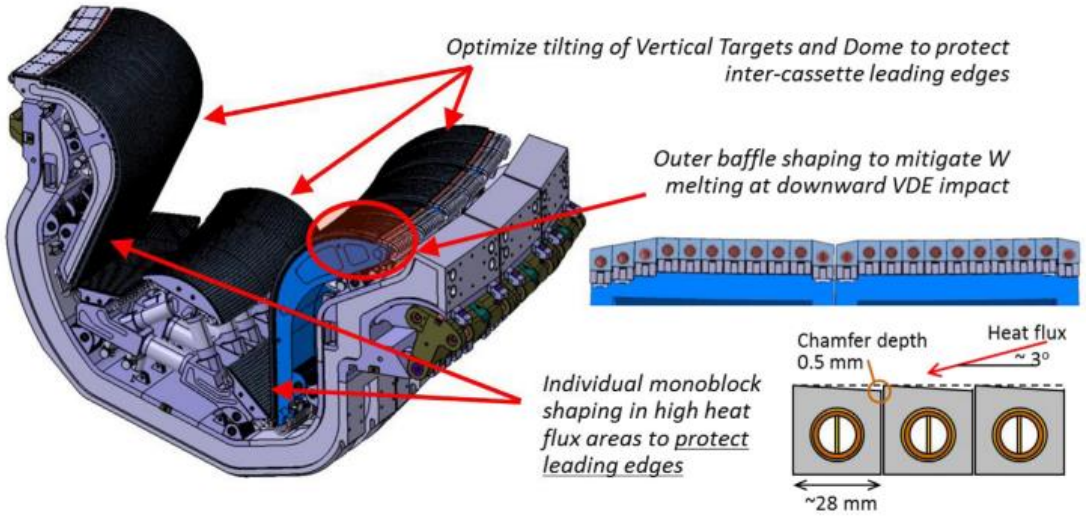


Figure 2 : ITER divertor & plasma facing component PFC design [2]

Focus on PFC lifetime under tokamak conditions

[1] iter.org
[2] Hirai T, Panayotis S, Barabash V, Amzallag C, Escourbiac F, Durocher A, et al. Use of tungsten material for the ITER divertor. Nuclear Materials and Energy. déc 2016;9:616-22.

Samples features & summary of irradiation/implantation conditions

Simpler microstructure !

	Samples features	ITER (expected)
Material	7x7x0,5mm^3 Tungsten sample	Tungsten monoblock **[9]**
Crystal type	**Monocrystal**	Polycrystal **[9]**
Purity	>99,999 %	99,94% [ref]
Temperature (°C)	~25 (RT)	1000-2000 at monoblock surface **[3]**
Damage Per Atom	~0,1 (W+ ions) / ~0,2-0,7 (3He+ ions)	~1 at divertor end life **[10]**
Helium fluence (at.m^{-2})	0 (W+ ions) / 2-3x10^{20} (3He+ ions)	10^{28-30} at divertor end life **[11]**

Figure 10 : Material & Irradiation features and comparison with ITER expected conditions

[3] Pitts RA et al. Physics basis for the first ITER tungsten divertor. Nuclear Materials and Energy. août 2019;20:100696.

[9] Missirlian, M. et al. The WEST project: Current status of the ITER-like tungsten divertor. Fusion Engineering and Design 89, 1048–1053 (2014).

[10] Bolt H, Barabash V, Federici G, Linke J, Loarte A, Roth J, et al. Plasma facing and high heat flux materials – needs for ITER and beyond. Journal of Nuclear Materials. déc 2002;307-311:43-52

[11] Ueda Y, Schmid K, Balden M, Coenen JW, Loewenhoff Th, Ito A, et al. Baseline high heat flux and plasma facing materials for fusion. Nucl Fusion. 1 sept 2017;57(9):092006.

Next goal : understand defects impact on microstructure during deformation approaching ITER operation conditions

	Samples features	ITER (expected)	To be studied
Material	7x7x0,5mm^3 Tungsten sample	Tungsten monoblock **[11]**	
Crystal type	**Monocrystal**	Polycrystal **[11]**	**Crystal orientation dependency ?**
Purity	>99,999 %	99,94%	Impurities impact ?
Temperature (°C)	~25 (RT)	1000-2000 at monoblock surface **[1]**	**High temperature effect ?**
Damage Per Atom	~0,1 (W+ ions) / ~0,2-0,7 (3He+ ions)	~1 at divertor end life **[12]**	**Higher dpa effect ?**
Helium fluence (at.m^{-2})	0 (W+ ions) / 2-3x10^{20} (3He+ ions)	10^{28-30} at divertor end life **[13]**	**Higher Helium fluence effect ?**

-Modelling to assess irradiation defects impact on dislocation motion

[1] Pitts RA et al. Physics basis for the first ITER tungsten divertor. Nuclear Materials and Energy. août 2019;20:100696.
[10] Jeong, J. & Voyiadjis, G. Z. A physics-based crystal plsticity model for the prediction of the dislocation densities in micropillar compression. *Journal of the Mechanics and Physics of Solids* **167**, 105006 (2022).
[11] Missirlian, M. et al. The WEST project: Current status of the ITER-like tungsten divertor. Fusion Engineering and Design 89, 1048–1053 (2014).
[12] Bolt H, Barabash V, Federici G, Linke J, Loarte A, Roth J, et al. Plasma facing and high heat flux materials – needs for ITER and beyond. Journal of Nuclear Materials. déc 2002;307-311:43-52
[13] Ueda Y, Schmid K, Balden M, Coenen JW, Loewenhoff Th, Ito A, et al. Baseline high heat flux and plasma facing materials for fusion. Nucl Fusion. 1 sept 2017;57(9):092006.

Next goal : understand defects impact on microstructure during deformation approaching ITER operation conditions

	Samples features	ITER (expected)
Material	7x7x0,5mm^3 Tungsten sample	Tungsten monoblock **[11]**
Crystal type	**Monocrystal**	Polycrystal **[11]**
Purity	>99,999 %	99,94%
Temperature (°C)	~25 (RT)	1000-2000 at monoblock surface **[1]**
Damage Per Atom	~0,1 (W+ ions) / ~0,2-0,7 (3He+ ions)	~1 at divertor end life **[12]**
Helium fluence (at.m^{-2})	0 (W+ ions) / 2-3x10^{20} (3He+ ions)	10$^{28-30}$ at divertor end life **[13]**

-Crystal orientation dependency ?

-Impurities effect ?

-High temperature effect ?

-Higher dpa effect ?

-Higher Helium fluence effect ?

-Modelling to assess irradiation defects impact on dislocation motion

[1] Pitts RA et al. Physics basis for the first ITER tungsten divertor. Nuclear Materials and Energy. août 2019;20:100696.
[10] Jeong, J. & Voyiadjis, G. Z. A physics-based crystal plsticity model for the prediction of the dislocation densities in micropillar compression. *Journal of the Mechanics and Physics of Solids* **167**, 105006 (2022).
[11] Missirlian, M. et al. The WEST project: Current status of the ITER-like tungsten divertor. Fusion Engineering and Design 89, 1048–1053 (2014).
[12] Bolt H, Barabash V, Federici G, Linke J, Loarte A, Roth J, et al. Plasma facing and high heat flux materials – needs for ITER and beyond. Journal of Nuclear Materials. déc 2002;307-311:43-52
[13] Ueda Y, Schmid K, Balden M, Coenen JW, Loewenhoff Th, Ito A, et al. Baseline high heat flux and plasma facing materials for fusion. Nucl Fusion. 1 sept 2017;57(9):092006.

Prospect : understand defects impact on microstructure during deformation approaching ITER operation conditions

	Samples features	ITER (expected)	To be studied
Material	7x7x0,5mm^3 Tungsten sample	Tungsten monoblock **[11]**	
Crystal type	**Monocrystal**	Polycrystal **[11]**	**Crystal orientation dependency ?**
Temperature (°C)	~25 (RT)	1000-2000 at monoblock surface **[1]**	**High temperature effect ?**
Damage Per Atom	~0,1 (W+ ions) / ~0,2-0,7 (3He+ ions)	~1 at divertor end life **[12]**	**Higher dpa effect ?**
Helium fluence (at.m^{-2})	0 (W+ ions) / 2-3x10^{20} (3He+ ions)	10^{28-30} at divertor end life **[13]**	**Higher Helium fluence effect ?**

[1] Pitts RA et al. Physics basis for the first ITER tungsten divertor. Nuclear Materials and Energy. août 2019;20:100696.
[10] Jeong, J. & Voyiadjis, G. Z. A physics-based crystal plsticity model for the prediction of the dislocation densities in micropillar compression. *Journal of the Mechanics and Physics of Solids* **167**, 105006 (2022).
[11] Missirlian, M. et al. The WEST project: Current status of the ITER-like tungsten divertor. Fusion Engineering and Design 89, 1048–1053 (2014).
[12] Bolt H, Barabash V, Federici G, Linke J, Loarte A, Roth J, et al. Plasma facing and high heat flux materials – needs for ITER and beyond. Journal of Nuclear Materials. déc 2002;307-311:43-52
[13] Ueda Y, Schmid K, Balden M, Coenen JW, Loewenhoff Th, Ito A, et al. Baseline high heat flux and plasma facing materials for fusion. Nucl Fusion. 1 sept 2017;57(9):092006.

Next goal : understand defects impact on microstructure during deformation

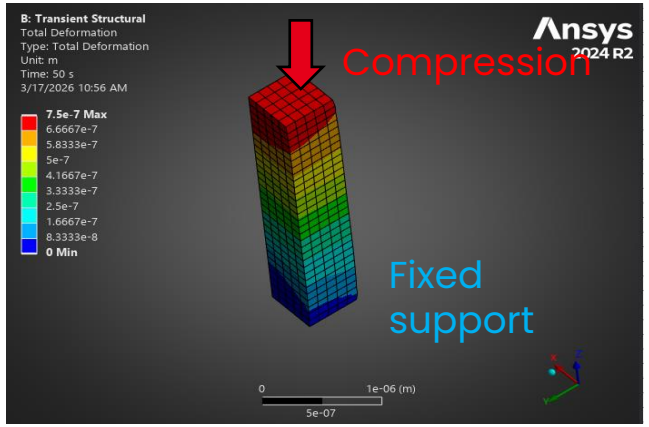


Figure 14: Ansys strain drived micro-pillar compression modelling

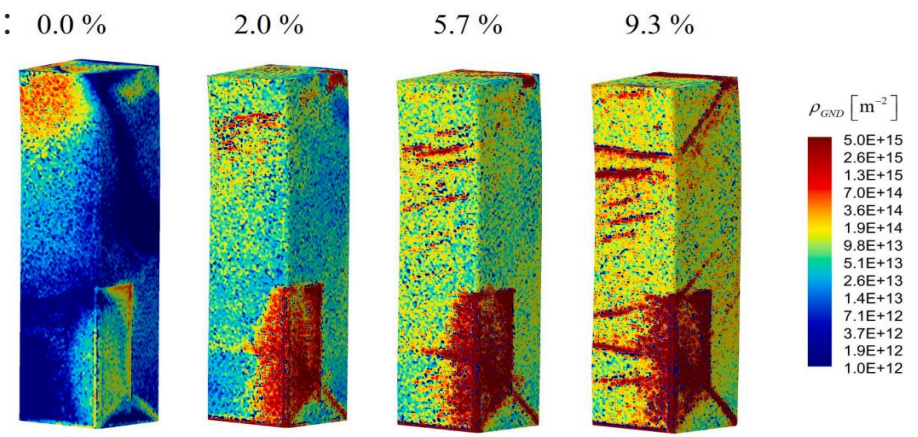


Figure 15: Example of GND dislocation assessment inside a micro-pillar during deformation using Crystal Plasticity Finite Element Modelling (CPFEM) [10]

-Modelling to assess irradiation defects impact on dislocation motion

	Samples features	ITER (expected)
Material	7x7x0,5mm^3 Tungsten sample	Tungsten monoblock **[11]**
Crystal type	**Monocrystal**	Polycrystal **[11]**
Purity	>99,999 %	99,94%
Temperature (°C)	~25 (RT)	1000-2000 at monoblock surface **[1]**
Damage Per Atom	~0,1 (W+ ions) / ~0,2-0,7 (3He+ ions)	~1 at divertor end life **[12]**
Helium fluence (at.m^{-2})	0 (W+ ions) / 2-3x10^{20} (3He+ ions)	10$^{28-30}$ at divertor end life **[13]**

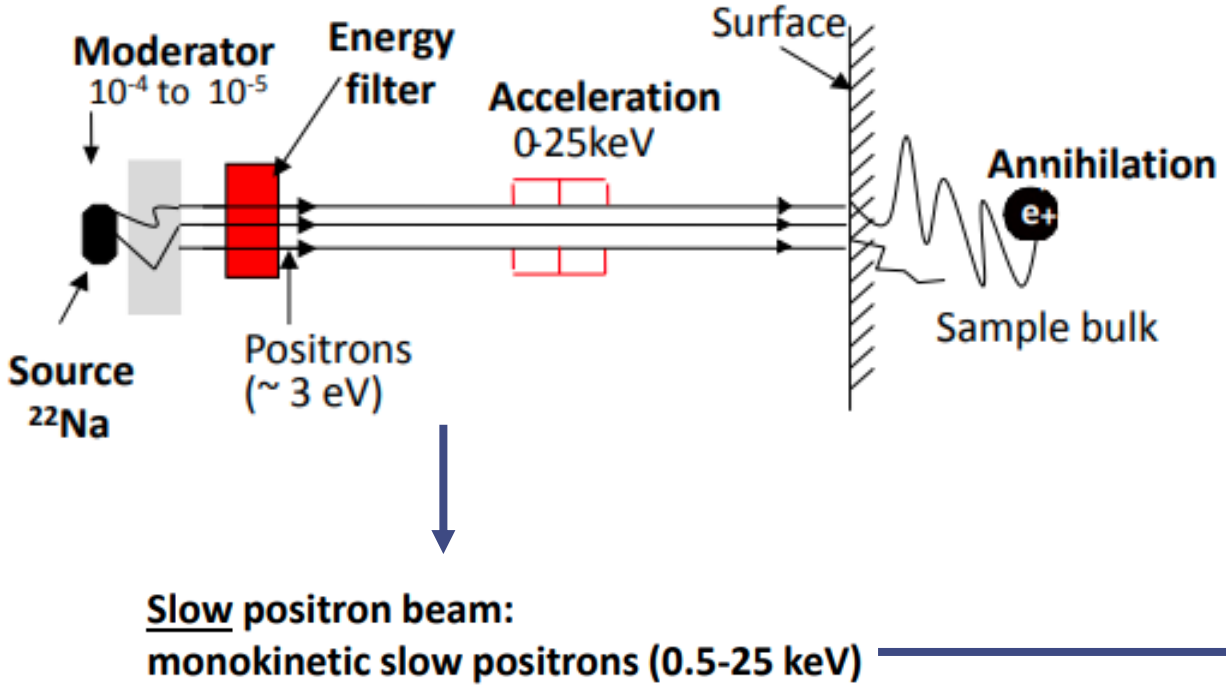
-Crystal orientation dependency ?
-Impurities effect ?
-High temperature effect ?
-Higher dpa effect ?
-Higher fluence influence ?

Anthony Flament

[1] Pitts RA et al. Physics basis for the first ITER tungsten divertor. Nuclear Materials and Energy. août 2019;20:100696.
[10] Jeong, J. & Voyiadjis, G. Z. A physics-based crystal plsticity model for the prediction of the dislocation densities in micropillar compression. *Journal of the Mechanics and Physics of Solids* **167**, 105006 (2022).
[11] Missirlian, M. et al. The WEST project: Current status of the ITER-like tungsten divertor. Fusion Engineering and Design 89, 1048–1053 (2014).
[12] Bolt H, Barabash V, Federici G, Linke J, Loarte A, Roth J, et al. Plasma facing and high heat flux materials – needs for ITER and beyond. Journal of Nuclear Materials. déc 2002;307-311:43-52
[13] Ueda Y, Schmid K, Balden M, Coenen JW, Loewenhoff Th, Ito A, et al. Baseline high heat flux and plasma facing materials for fusion. Nucl Fusion. 1 sept 2017;57(9):092006.

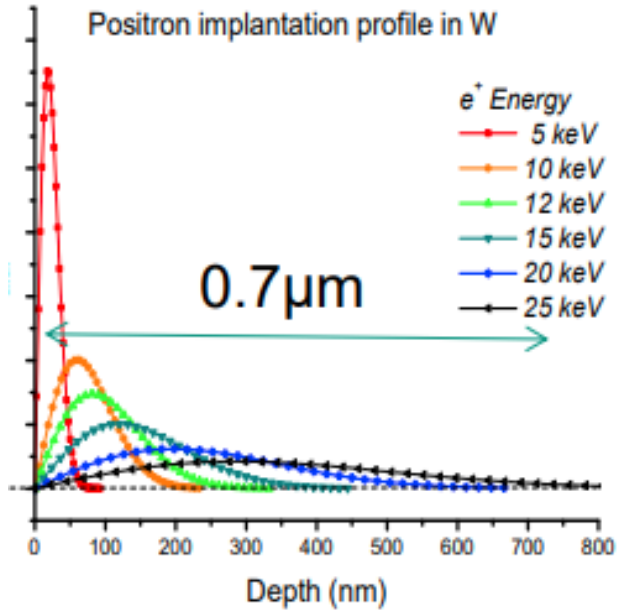
Doppler broadening Positron Annihilation Spectrocscopy (PAS), or how to probe vacancy defects & free volumes using lattice electronic structure

Figure 19: DB-PAS principle [12]



Slow positron beam:
monokinetic slow positrons (0.5-25 keV)

Figure 20: Positron implantation profile in W for 5 to 25 keV



Thin layers

[12] Marie-France Barthe, Positron Annihilation Spectroscopy to Characterize Irradiation Induced Vacancy Type Defects in Materials for Nuclear Fission and Fusion, EPJ Web of Conferences 115, 03004 (2016) DOI: 10.1051/epjconf/201611503004, https://www.epj-conferences.org/articles/epjconf/pdf/2016/10/epjconf_MINOS2015_03004.pdf